FINITE ELEMENT MODELING OF MACHINING PARTICLE REINFORCED ALUMINUM METAL MATRIX COMPOSITES

A MASTER'S THESIS

in

Manufacturing Engineering

Atılım University

by

NAKKA LOTFY RAKE

JULY 2018

FINITE ELEMENT MODELING OF MACHINING PARTICLE REINFORCED ALUMINUM METAL MATRIX COMPOSITES

A THESIS SUBMITTED TO

THE GRADUATE SCHOOL OF NATURAL AND APPLIED SCIENCES

OF

ATILIM UNIVERSITY

BY

Nakka Lotfy Rake

IN PARTIAL FULFILLMENT OF THE REQUIREMENTS

FOR

THE DEGREE OF MASTER OF MANUFACTURING ENGINEERING

July, 2018

Approval of the Graduate School of Natural and Applied Sciences, Atılım University.

_____

Prof. Dr. Ali Kara

Director

I certify that this thesis satisfies all the requirements as a thesis for the degree of Master of Science.

_____

Prof. Dr. Sadık Engin Kılıç

Head of Department

This is to certify that we have read the thesis "FINITE ELEMENT MODELING OF MACHINING PARTICLE REINFORCED ALUMINUM METAL MATRIX COMPOSITES" submitted by "Nakka Lotfy Rake" and that in our opinion it is fully adequate, in scope and quality, as a thesis for the degree of Master of Science.

_____	_____
Asst. Prof. Dr. Samad Nadimi Bavil Oliaei	Prof. Dr. Sadık Engin Kılıç
Co-Supervisor	Supervisor

Examining Committee Members

Prof. Dr. Sadık Engin Kılıç _____

Doç. Dr. H. Özgür Ünver _____

Asst. Prof. Dr. Bahram Lotfi Sadigh _____

Date: 11 June 2018

I declare and guarantee that all data, knowledge and information in this document has been obtained, processed and presented in accordance with academic rules and ethical conduct. Based on these rules and conduct, I have fully cited and referenced all material and results that are not original to this work.

Name, Last name:Nakka Lotfy Rake

Signature:

ABSTRACT

FINITE ELEMENT MODELING OF MACHINING PARTICLE REINFORCED ALUMINUM METAL MATRIX COMPOSITES

Nakka Lotfy Rake

M.S., Manufacturing Engineering Department

Supervisor: Prof. Dr. Sadık Engin Kılıç

Co-Supervisor: Asst. Prof. Dr. Samad Nadımi Bavil Oliaei

July 2018, 71 pages

Metal matrix composites (MMCs) have become key materials in many technical fields, including automotive, aerospace and nuclear power plants. In most of these applications, machining processes are required to achieve the desired characteristics of the final product. Therefore, it is important to study the machining of MMCs and develop process models to understand their behavior during machining operations. Based on process models, machining quality and cost can be improved by optimizing the cutting conditions for specific MMCs. As a step towards this goal, finite element modeling (FEM) is used to study the machining of particulate aluminum metal matrix composites (p-Al-MMCs). The selected matrix material was aluminum alloy A359 reinforced with silicon carbide (SiC) particles having a diameter of 20 μm with a volume fraction of 20%. Orthogonal cutting of p-Al-MMC has been studied by three different approaches. In the first approach attempt has been made to implement an equivalent homogeneous material model (EHM), while in the second and third approaches p-Al-MMC is modeled as a two-phase heterogeneous material. The second and third approaches rely on periodic square and periodic hexagonal distributions of reinforcement particles, respectively. The interaction between matrix/cutting tool, matrix/reinforcement and reinforcement/ cutting tool has been considered. The results of FE simulations are compared with the experimental data available in the literature. The results revealed that, EHM models calibrated using high strain rate tests may not be able to give good predictions of cutting forces and they should be re-calibrated for machining simulations. The results also revealed that, by modeling p-MMCs as a heterogeneous material the accuracy of cutting force predictions can be improved significantly.

Keywords: Finite Element Modeling, orthogonal cutting, particle reinforced aluminum metal matrix composite, heterogeneous material, tool-workpiece interaction.

ÖZ

PARTİKÜL TAKVİYELİ ALÜMİNYUM METAL MATRİS KOMPOZİT MALZEMELERİN TALAŞLI İŞLENMESİNİN SONLU ELEMANLAR YÖNTEMİYLE MODELLENMESİ

Nakka Lotfy Rake

M.S., İmalat Mühendisliği Bölümü

Tez danışmanı: Prof. Dr. Sadık Engin Kılıç

Eş Tez Danışmanı: Dr. Öğretim Üyesi Samad Nadimi Bavil Oliaei

Temmuz 2018,71 sayfa

Metal matris kompozitleri (MMC'ler) otomotiv, havacılık ve nükleer santraller gibi birçok teknik alanda önemli malzemeler haline gelmiştir. Bu uygulamaların çoğunda, nihai ürünün istenen özelliklerine ulaşmak için talaşlı işleme süreçleri gereklidir. Bu nedenle, MMC'lerin talaşlı işlemesini incelemek ve işleme operasyonları sırasında davranışlarını anlamak için süreç modellerini geliştirmek önemlidir. Proses modellerine dayanarak, belirli MMC'lerin kesme koşullarını optimize ederek talaşlı işleme kalitesi ve maliyeti iyileştirilebilir. Bu hedefe doğru bir adım olarak, partikül takviyeli alüminyum metal matris kompozitlerinin (p-Al MMC'ler) talaşlı işlenmesini incelemek için sonlu eleman modellemesi (FEM) kullanılır. Seçilen matris malzemesi,% 20'lik bir hacim fraksiyonu ile 20 µm çapa sahip silikon karbür (SiC) parçacıkları ile güçlendirililmiş alüminyum alaşımı A359'dur. P-Al-MMC'nin ortogonal kesimi üç farklı yaklaşımla incelenmiştir. Birinci yaklaşımda, eşdeğer bir homojen malzeme modeli (EHM) uygulanmaya çalışılırken, ikinci ve üçüncü yaklaşımlarda p-Al-MMC, iki fazlı bir heterojen malzeme olarak modellenmiştir. İkinci ve üçüncü yaklaşımlar sırasıyla donatı parçacıklarının periyodik karesi ve periyodik altıgen dağılımlarına dayanmaktadır. Matris / kesici takım, matris / takviye ve takviye/kesme aleti arasındaki etkileşim göz önüne alınmıştır. FE simülasyonlarının sonuçları literatürdeki deneysel veriler ile karşılaştırılmıştır. Sonuçlar, yüksek gerilme oranı testleri kullanılarak kalibre edilen EHM modellerinin kesme kuvvetlerinde iyi tahminler veremeyebileceğini ve talaşlı işleme simülasyonları için yeniden kalibre edilmesi gerektiğini ortaya çıkarmıştır. Sonuçlar ayrıca, p-MMC'lerin heterojen bir materyal olarak modellenmesiyle, kesme kuvveti tahminlerinin doğruluğunun önemli ölçüde geliştirilebileceğini ortaya koymuştur.

Anahtar Kelimeler: Sonlu Elemanlarla Modelleme, ortogonal kesim, partikül takviyeli alüminyum metal matris kompozit, heterojen malzeme, takım-iş parçası etkileşimi.

With love

To my parents: Lotfy Rake and Sanaa Najeeb

ACKNOWLEDGMENTS

I cannot express enough thanks to all of those who continued to support and encourage me to complete this thesis.

I would like to thank my supervisor Prof. Dr. Sadık Engin Kılıç with my sincere appreciation for his excellent help, guidance and support throughout my study.

I would like to express my deep appreciation to my co-supervisor Dr. Samad Nadimi Bavil Oliaei for his guidance, patience, support and encouragement. This support led me to continue to solve the difficult stages during this study.

I would like to thank the Department of Manufacturing Engineering, as well as the Metal Forming Center of Excellence at Atilim University for financing and sponsoring this research.

I would like to thank my friends for helping me in this research: Pouya Zoghipour, Sinan Akbulut, Dr. Adnan Al-Umary, and Dr. Kakhum Abed.

I would like to thank my husband and children for their love and encouragement.

Finally, my heartfelt gratitude to my parents, brothers and sisters for their unconditional love and support for me to achieve better.

TABLE OF CONTENTS

LIST OF TABLES

TABLE

LIST OF FIGURES

FIGURES

LIST OF ABBREVIATIONS

Al-MMCs	Aluminum metal matrix composites
BUE	Built Up Edge
EHM	Equivalent homogenous material
FEM	Finite Element Modeling
PRMMC	Particulate reinforced metal matrix composite
p-Al-MMCs	Particulate aluminum metal matrix composites

CHAPTER 1

INTRODUCTION

1. Introduction

The developments in the industry and technology have pushed engineers and scientists to search for and develop new types of materials which have to satisfy challenging requirements like high stiffness and high corrosion and wear resistance.

The wide use of aluminum alloys in manufacturing, aerospace and automobile sectors is well recognized today. Aluminum alloys have desirable properties such as high strength, light weight, exceptional corrosion resistance, and high machinability in addition to the low cost of this material.

Aluminum alloys cannot meet all engineering requirements. For instance, these alloys have a low wear resistance. To solve this problem, new engineering materials are developed by reinforcing aluminum alloys with ceramic particles. These are known as particulate aluminum metal matrix composites (p-Al-MMCs). The superior properties of MMCs include high stiffness, thermal stability, wear and corrosion resistance. MMCs have become key materials in many technical fields, including nuclear power stations and in aerospace. They are also used in the automotive industry for manufacturing engine connecting rods, propeller shafts, brake discs, etc. Aluminum alloy reinforced with either SiC or Al_2O_3 are commonly used because of their availability and enhanced mechanical properties.

Machining processes are required to achieve the desired specifications of the final product. Ceramic reinforcements in MMCs cause difficulties while machining. Ceramic particles have the same base material as the cutting tools.

Based on the process model, machining quality and cost can be improved by optimizing the cutting conditions for specific composite materials. As a step

towards this goal, Finite Element Modeling will be used in this study to machine particulate aluminum metal matrix composites (p-Al-MMCs). FEM development provides various scenarios to understand the interactions between the cutting tool and particles and find the effect of cutting parameters on MMC behavior during a machining operation.

Machining MMCs is considered to be a challenging process. The main part of understanding any type of machining process lies in obtaining a model to predict machining forces. A cutting force is an excellent tool for studying the relationships between various aspects of the process, such as tool wear and damage in the work piece material.

1.1 Objectives

This research aims to provide a clear understanding of machining particulate metal matrix composites. This understanding will be achieved through a numerical modeling of the process.

The type of numerical model will be finite element modeling (FEM). This model simulates the behavior of a matrix, particles and the interactions between the matrix and particles as well as interactions between the MMC and the cutting tool.

In this study, an attempt is made to use constitutive models that best describe the metal matrix composite material response during the cutting process. The results of the FE simulations are compared with experimental data from the literature review.

1.2 Scope of the thesis

Chapter 1 presents the introduction, objectives and the aim of this study.

Chapter 2 presents the background topics and a literature review relevant to this thesis.

Chapter 3, Research Methodology, presents the research motivation, research procedure, and methodology.

Chapter 4 presents details of the finite element method and explains the important criteria that should be achieved in this model. These criteria are used to simulate four models.

In the first model, two approaches are used. FEM is used to simulate the machining of aluminum alloy 6061 under different cutting conditions to understand the effects of these conditions on machining. FEM are comparable with experimental results to determine the accuracy of this numerical method. In the second approach, FEM is used to simulate the machining of aluminum alloy with different cutting tool geometries while the cutting condition remains the same in order to find the effects of cutting tool geometry on machining results.

Model II, Model III and Model IV, these three models have been used to describe the behavior of p-Al-MMCs while machining. The matrix material selected was aluminum alloy A359 reinforced with silicon carbide (SiC) particles having a diameter of 20 μm with a volume fraction of 20%.

Model II uses FEM to simulate the machining of MMCs reinforced with particles as an equivalent homogenous material (EHM) where the plastic deformation and damage evolution are governed by high-strain rate deformation behavior of a A359/SiC/20p composites and Johnson-Cook damage models, respectively.

Model III uses FEM to simulate MMCs as a heterogeneous material with periodic square particle distributions.

Model IV uses FEM to simulate MMCs as being heterogeneous with periodic hexagonal particle distributions.

All three simulations of MMCs are presented and compared with experimental results.

Chapter 5 presents the findings and conclusions of this thesis. Possible future work in this field is also described.

CHAPTER 2

2. BACKGROUND OF THE STUDY AND LITERATURE REVIEW

2.1. Introduction

The final shape of most mechanical components is obtained by machining operations. Unwanted material is removed. The machining process achieves high dimensional accuracy, certain shapes and surface integrity [1].

Metal cutting is chip formation via the interaction of a cutting tool wedge with the work piece surface. This is achieved through relative movement between them. Even though all metal-removing operations share the same mechanical principle, geometries and kinematics vary for each machining process. In order to build solid and reliable simulations, it is essential to understand this mechanical principle, often converted into mechanical numerical models.

2.2 Orthogonal and oblique metal cutting

2.2.1 Orthogonal metal cutting

Orthogonal cutting is the simplest of the material removing processes. In orthogonal cutting, the material is removed with a cutting edge that is perpendicular to the direction of the of relative tool-work piece motion, as seen in Figure 2.1.

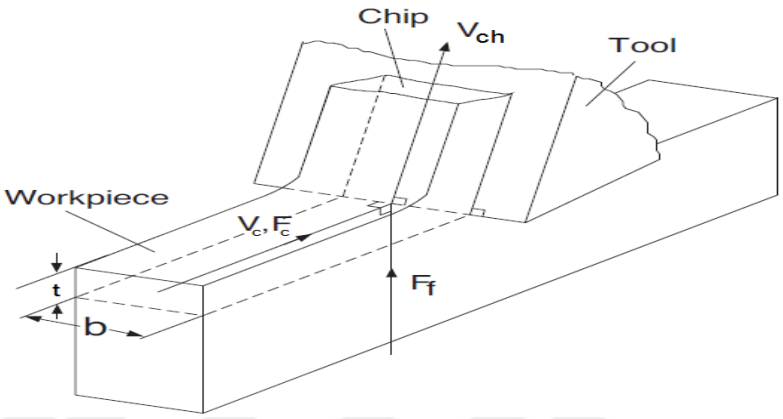

Figure 2.1: Orthogonal cutting geometry

Figure 2.1 shows the width of the cut (b) and the uncut chip thickness (t). The material is removed from the work piece by shear force. Since it is a two-dimensional plane strain deformation process without side spreading of material along the cutting edge, the cutting force is only in the direction of the cutting velocity. The forces F_c and F_f are called the cutting and feed forces, respectively. The chip is plastically deformed in the primary deformation zone. The shear angle ϕ defines its inclination. The secondary deformation zone is characterized by a sticking region at the tool-chip interface and sliding region. The sticking region is closer to the edge of the tool, where the cutting causes shear stresses on the chip. The sliding region, where the chip slides, is located above the previous region. The primary deformation zone is closely related to severe plastic deformation, while the secondary deformation zone is related to the friction, as shown in Figure 2.2 [1].

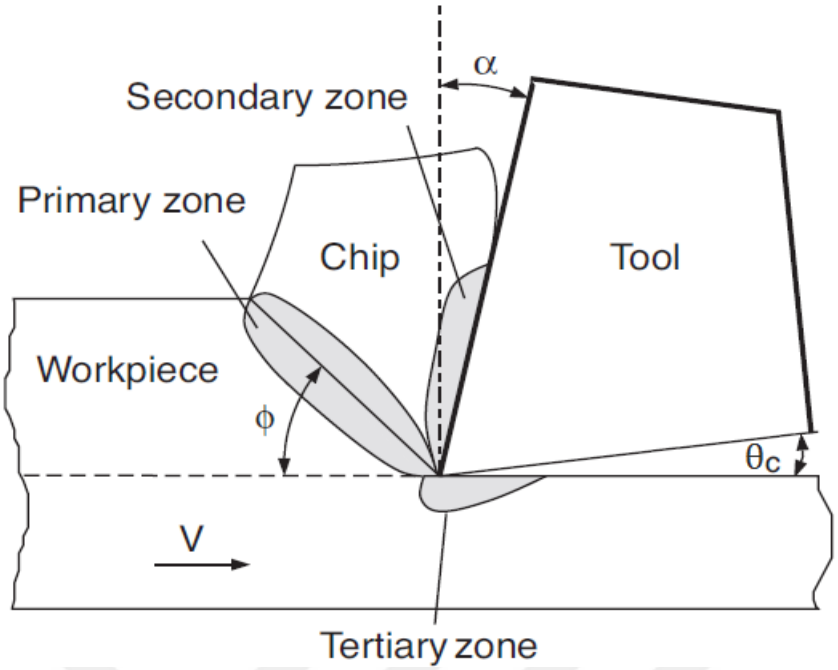

Figure 2.2: Deformation zones in orthogonal cutting cross-section scheme [1]

There are three important angles in orthogonal cutting: the rake angle (α), which determines the direction of the chip flow as it forms. This angle takes different values: negative, zero and positive (Note the positive rake angle in Figure 2.2).

The clearance angle (θ_c) provides a small clearance between the tool flank and the transient cut surface, which helps to protect the flank from abrasion [2-4].

2.2.2 Oblique metal cutting

In oblique cutting (see Figure 2.3), the cutting edge is oriented at an inclination angle (λ) and the third force acts in the radial direction (F_r). This inclination allows forces to act on a larger area, which will decrease tool wear. However, for analysis and modelling purposes, oblique cutting is more complex than orthogonal cutting. Despite certain machining processes being more realistic through oblique cutting, it does not submit improvement of the metal cutting analysis [3].

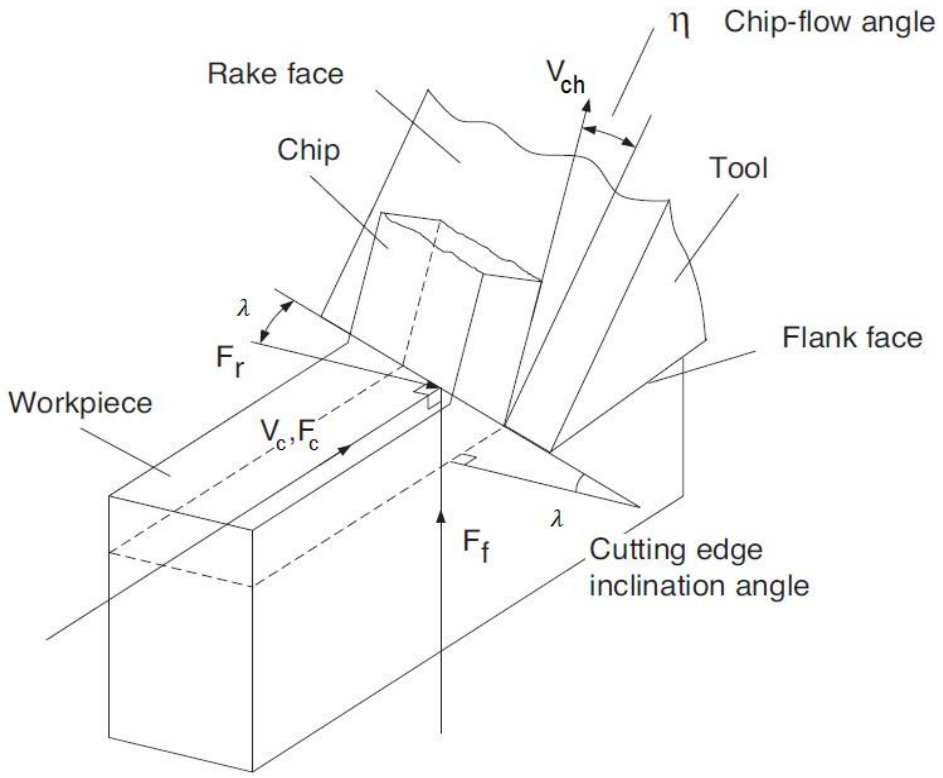

Figure 2.3: Oblique cutting geometry

2.3 Chip Formation

The chip formation in cutting is approximately identical between oblique and orthogonal cutting. There are three types of chip that occur in machining operations: discontinuous chips, continuous chips and continuous chips with BUE [5], figure 2.4.

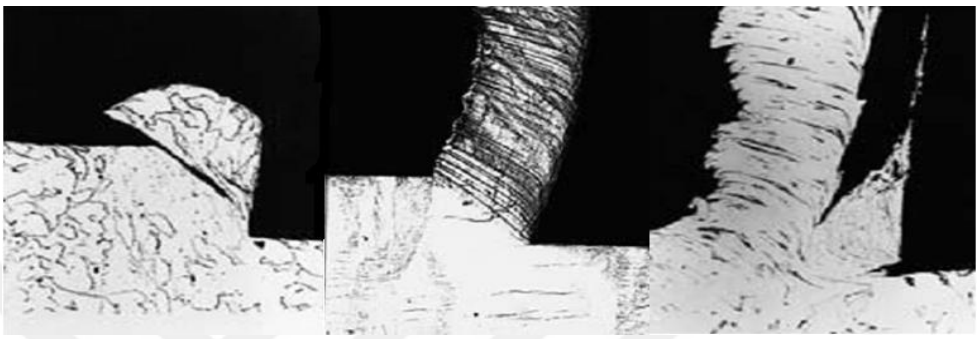

(a) (b) (c)

Figure 2.4 [5] : Chip types: (a) Discontinuous, (b) Continuous, (c) Continuous with BUE

Discontinuous chips occur when brittle metals are machined or when some ductile metals are machined at low cutting speeds. Machine vibration or tool chatter may cause these types of chip to form.

Continuous chips occur when ductile metals are cut at high speeds. This type of chip is considered ideal for cutting operations because it results in a better surface finish. Built up edge (BUE) occurs when workpiece material adheres to the tool cutting edge, affecting the chip formation. High temperature and pressure conditions as well as high friction in the tool-chip interface may cause BUE to happen and to grow during the machining process [5].

2.4. Friction in Metal Cutting

In metal cutting, friction between the chip and tool interface plays a significant role in important process variables, such as temperature and tool wear. Therefore, it has to be studied in detail. The laws of friction were first

determined by Leonardo da Vinci and later restated by Amonton and Coulomb. According to these laws, the friction force is proportional to the normal force, which means that the coefficient of friction is constant. The friction force and the coefficient of friction are independent of the apparent area of the sliding interface. In metal cutting, friction conditions are very different from a simple dry friction; the normal force is very high.

Friction in metal cutting has been studied in detail by many researchers, who studied the contact and friction stresses on the rake face by using direct measurements. Usui and Takeyama (1960) measured the distribution of the shear (τ) and the normal (σ) stresses on the rake face of the tool. As shown in Figure 2.5, they found that the shear stress remains constant over about half of the tool-chip contact nearest the cutting edge, but it decreased to zero over the remainder, reaching zero at point C where the chip breaks contact with the tool. The normal stress was found to decrease and reach zero from the cutting edge to point C. Zorev (1963) found also similar results from his experiments.

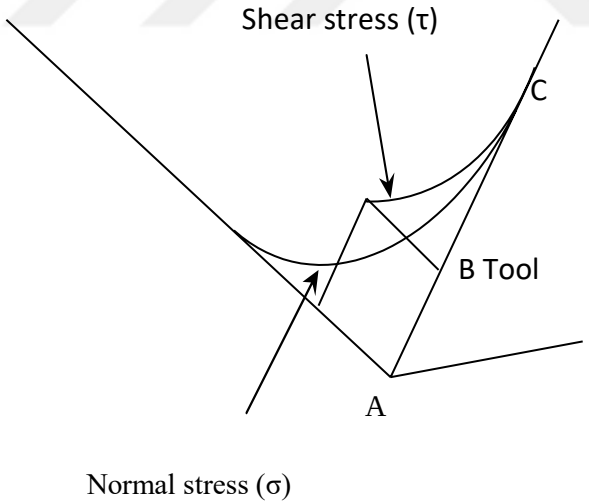

Figure 2.5: Distribution of shear and normal stresses on the rake face [6]

Over the length AB, normal stress is sufficiently high, the contact area to total area ratio approaches unity and the metal adheres to the rake face. This region is called the sticking region and plastic deformation occurs in the chip. The coefficient of friction in the sticking region is not constant, and it depends on the magnitude of the normal load. The value of the coefficient

of friction in this region is lower than the value under sliding friction conditions. In the length from B to C, which extends from the end of the sticking region to the point where the chip loses contact with the tool rake face, the contact area to total area ratio is less than unity, so the coefficient of friction is constant and sliding friction occurs.

The measured coefficient of friction in metal cutting is an average value based on both regions. Any changes in cutting conditions that may change lengths AB and BC will change the value of the coefficient of friction.

2.5 Shear Stress in Metal Cutting

The shear stress in metal cutting is higher than the yield stress of determined from tensile test on work materials. Rubbing effect and the pre-flow region existence are two reasons of this situation. Rubbing effect on the clearance of the tool introduces a force which is measured but does not contribute to the shearing process. Secondly, a pre-flow region is present in most of the cutting processes that extends the length of the shear plane that assumed in analysis, as shown in Figure 2.6.

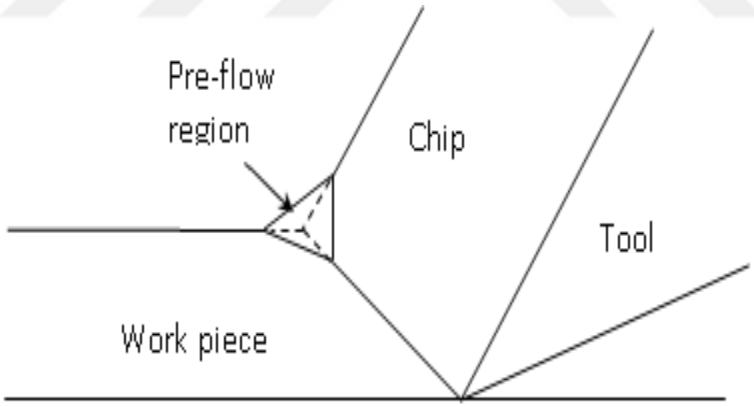

Figure 2.6: Pre-flow region

In addition to these two reasons, high normal stress can increase the yield shear stress on the shear plane during cutting. At low cutting speeds, work hardening of the material must also be taken into account while determining the shear stress. The strain rate and temperature normally cause opposing effects on the yield stress of the material. Since both the strain rate and temperature are relatively high in metal cutting operations, sometimes it can be assumed that they cancel each other; however, recent considerations of

the mechanism of the yield at very high strain rates indicate that the high strain rate may have the effect of increasing yield stress above the static yield value [7].

2.6 Temperature in Metal Cutting

Temperature has a significant effect on the performance of a cutting tool and the quality of the machined component and its determination is essential when it comes to estimate tool wear [8]. The heat generated in metal cutting was one of the first investigated topics in machining [9].

During a metal cutting operation, high temperatures are generated because of plastic deformation of the work piece material and friction along the tool/chip interface. The determination of temperatures in the tool, chip and work piece is important for process efficiency because these temperatures have a great influence on the rate of tool wear, strength of the work piece material, the mechanics of chip formation, surface integrity, cutting forces, etc.

Heat sources in metal cutting are shown in Figure 2.7. In cutting, nearly all of energy dissipated in plastic deformation is converted into heat that in turn raises the temperature in the cutting zone. Since the heat generation is closely related to the plastic deformation and friction, we can specify three main sources of heat when cutting:

a. Plastic deformation by shearing in the primary shear zone (heat source Q1)

b. Plastic deformation by shearing and friction on the cutting face (heat source Q2)

c. Friction between chip and tool on the tool flank (heat source Q3)

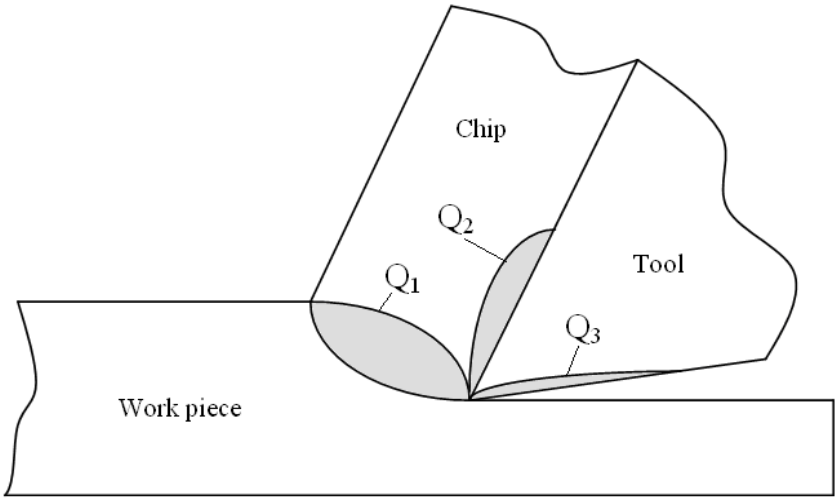

Figure 2.7: Locations of heat sources in metal cutting [9]

2.7 Metal matrix composites (MMCs)

The mixture of two or more different types of material in which all the mixed materials retain their physical and chemical identities is called a composite [10]. The phase which forms a continuous network and which surrounds the other phases is called a matrix, whereas the discontinuous and dispersed phase is called the reinforcement.

Metal Matrix Composite materials (MMCs) have been applied in numerous fields, such as the energy, defense, aerospace, bio-technology, optics and automobile fields, because of their reinforced high performance mechanical properties and reduced weight. In recent decades, substantial progress has been achieved in the development of MMCs. Figure 2.8 shows some macroscale applications.

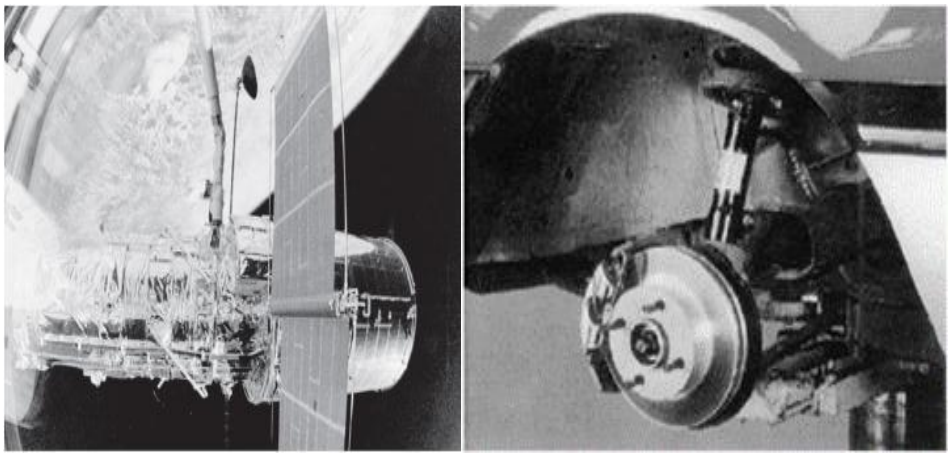

(a) (b)

(a) P100/6061 Al high-gain antenna wave [10]

(b) Vented passenger car brake disk [11]

Figure 2.8: Macro-scale applications of advanced MMCs

The light weight and high toughness of aluminum-makes it a very good matrix in MMCs. The ceramic particle reinforcement significantly improves the mechanical properties of wear resistance and strength. These properties of composite metals make them better than alloys. The strength of particle-reinforced composites is observed to be most strongly dependent on the volume fraction and particle size of the reinforcement.

Performance of a composite depends on:

a. The properties of the matrix and reinforcement

c. The size and distribution of constituents

d. The shape of the constituents

e. The nature of the interface between constituents

2.7.1 Types of MMC

Composites are classified into two types:

a. on the basis of the matrix material.

b. on the basis of filler material.

2.7.1.1 On the basis of matrix material

a. Ceramic Matrix Composites (CMC):

This class of composites contains ceramic materials as the matrix phase. CMCs have been developed primarily to improve the fracture toughness of ceramic materials. This finds the CMCs being used in extreme environments of high temperature and stress states. The dispersed phase plays a major role in preventing the propagation of cracks. This dispersed phase can be fibers, particles or whiskers [12].

b. Polymer Matrix Composites (PMC):

These contain a polymer as the matrix phase and fibers such as e-glass, carbon or aramid as the reinforcing phase [12]. Varieties of Polymer-Matrix Composite (PMC) are mostly used in Glass Fiber-Reinforced Polymer (GFRP) composites, Carbon Fiber-Reinforced Polymer (CFRP) composites and Aramid Fiber-Reinforced Polymer Composites. The most commonly used polymers as a matrix are vinyl esters and polyesters. PMCs are widely used based on their properties and ease of fabrication.

c. Metal Matrix Composites (MMC):

The matrix phase for MMC is a metal which is often ductile. MMCs are manufactured to have high strength to weight ratios, high resistance to abrasion and corrosion, resistance to creep, good dimensional stability, and high temperature operability. MMCs are used in industries such as automotive and aerospace industries. Mainly aluminum and copper are used as the metal matrix. Composite degradation may be a problem while using MMCs at elevated temperatures. To avoid this, the reinforcement is either given a protective surface coating or the composition of the matrix alloy is modified [12].

2.7.1.2 On the basis of filler materials

There are four main types of MMC depending on the distribution of the reinforcement, as shown in Figure 2.9.

1. Particle-reinforced MMCs
2. Short fiber- or whisker-reinforced MMCs
3. Continuous fiber- or sheet-reinforced MMCs
4. Laminated or layered MMCs

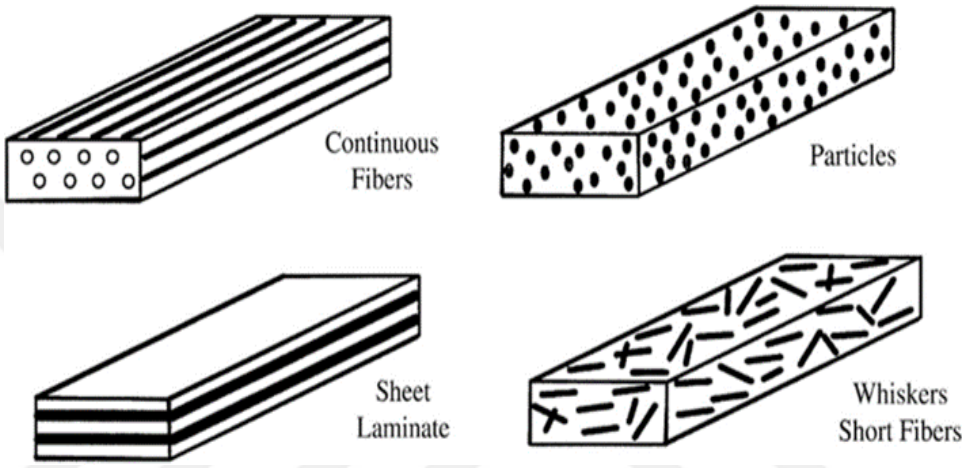

Figure 2.9: Classification of Metal Matrix Composites on the basis of reinforcements [13].

2.8 SiC Particulate Reinforced with Aluminum Metal Matrix Composites

Particulates are the most common and cheapest reinforcement materials. These produce the isotropic property of MMCs, which shows a promising application in structural field.

Aluminum matrix composites are potential materials for various applications due to their good physical and mechanical properties. The addition of reinforcements into the metallic matrix improves the stiffness, specific strength, wear, creep and fatigue properties compared to conventional engineering materials [14].

Stiffness and strengths of particulate-reinforced aluminum MMCs are significantly better than those of the aluminum alloy matrix. For example, at

a volume fraction of 40 percent silicon carbide particulate reinforcement, the strength is about 65 percent greater than that of the 6061-aluminum matrix, and the stiffness is doubled [15].

In the particulate reinforced composite, the size of the particulate is more than 1 μm, so it strengthens the composite in two ways, the first of which is that the particulate carries the load along with the matrix materials and the other way is by formation of an incoherent interface between the particles and the matrix. Therefore, a larger number of dislocations is generated at the interface and the material is strengthened. The degree of strengthening depends on the amount of particulate (volume fraction), distribution, size and shape of the particulate [15].

The reinforcement distribution also influences the ductility and fracture toughness of the MMC and hence indirectly the strength [16]. A uniform reinforcement distribution is essential for effective utilization of the load carrying capacity of the reinforcement. Non-uniform distributions of reinforcement in the early stages of processing has been observed to persist to the final product in the forms of streaks or clusters of infiltrated reinforcement with their attendant porosity, all of which lowered the ductility, strength and toughness of the material [17].

Al-MMCs have high stiffness (high strength/modulus and low density) are widely used in the manufacturing industries, mainly in aircraft, aerospace, automotive and various other fields [18].

The most commonly used reinforcement is silicon carbide (SiC). The SiC reinforcement increases the tensile strength, hardness and wear resistance of aluminum and its alloys. The particle distribution plays vital role in the properties of the Al-MMC.

The volume fraction of SiC can be varied to have a coefficient of thermal expansion compatible with other parts of the system assembly [19].

Finally, they are cheap when compared with other low-density alloys (such as Mg or Ti) [20].

2.9 Literature Review

The development of metal cutting theory was reviewed in detail by Finnie who reported that the earliest documented research in metal cutting. Cocquilhat measured the work required to remove a given volume of metal in drilling. Finnie further reported that the first attempts to explain chip formations were made by Time and by Tresca in 1870-1873 [21]. Taylor, in his pioneering work on metal cutting, reported the results of 26 years to investigate the effect of tool materials and cutting conditions on tool life during roughing cuts [21]. His discovery of the empirical law governing the relationship between cutting speed and tool life is still used and has been employed as the basis for much research in machining. Many researchers have published their work to explain the complex behavior at the tool/work piece interface [22] [23]. Ernest and Merchant was the first who developed the simplest and most widely used model for cutting in 1941[24].

Ceramic-reinforced Metal Matrix Composites (MMCs) will replace light-weight metallic materials such as magnesium, aluminum and their alloys. MMCs have a high mechanical performance with higher stiffness [25].

Researchers in the field of metal cutting have developed an analysis of the cutting process that provides a clear understanding of the mechanisms involved. Some of the studies focus on analysis and others focus on the experimental field.

In an experimental study, Xia et al. sought to find the fracture behavior of MMCs reinforced with micro-sized ceramic particles (alumina and SiC) [26]. The size of ceramic particles was 15~30 μm and the volume fractions were 5%~20%. The matrix materials used, an aluminum alloy (2618, 6061 and 7075 Al), were examined under three-point bending tests. The results revealed that the energy absorption level during cracking depended on both matrix strength and ductility.

Kannan et al. carried out research to understand the role of the ductile matrix on machining performance by estimating line defects (Figure 2.10) resulting from the turning operation for alumina reinforced Al-MMCs. The ceramic

particle size was 0.25 µm with two types of aluminum alloy (7075 and 6061) [27].

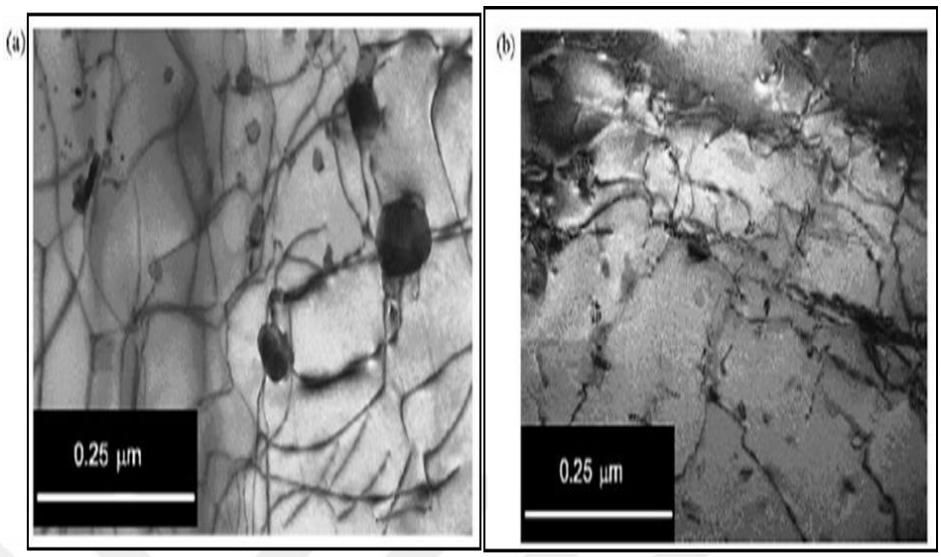

Figure 2.10: Line defects in the two types of aluminum alloy matrix: (a) Al-7075/10% alumina MMC, and (b) Al-6061/10% alumina MMC [27]

Pramanik et al. experimentally studied the effects of reinforcement particles on the machining performance of Al-MMCs. The SiC particle size was 6-18 µm and the type of process was turning under dry conditions. The effect of the ceramic particles on the cutting forces, surface roughness, chip shape, shear angles and friction angles were examined. The results revealed a large variation of cutting force for the Al-MMCs [28].

In particulate MMCs, factors of particle shape, particle size and volume fraction have a great effect on the machinability of particulate MMCs. Therefore, these factors require further study in order to better understand the machining of MMCs.

Some studies discuss the difficulties of machining MMCs and suggest that "the more widespread usage of particular aluminum matrix composites is significantly impeded by their poor machinability" [29].

The experimental approach to studying machining processes is expensive and time consuming, especially in metal cutting when a wide range of parameters include tool geometry, materials, cutting conditions, and so on.

Because of these difficulties, alternative approaches have been developed as mathematical simulations where numerical methods are used.

Grzesik defined a model as an abstract system which is equivalent to the real system and its build is the properties and characteristics of a real system [30]. A model is used to investigate, calculate and explain for demonstration purposes. A model allows us to understand the behavior of a reality section [31].

The finite element method has been used in modelling orthogonal (2D) and oblique (3D) metal cutting. The first finite element model for metal cutting processes was developed by Klamecki [32], who used an updated Lagrangian elastic-plastic with a three-dimensional model. This model was limited to the initial stages of chip formation. Usui and Shirakashi developed the first two-dimensional FE orthogonal machining simulation. They applied a special computation method called the iterative convergence method to obtain solutions for steady state cutting [33].

Ceretti et al. developed a cutting model by deleting elements having reached a critical value of accumulated damage [34].

Chuzhoy et al. proposed an FE model for the orthogonal cutting of ductile iron [35]. Different phases of iron were used in this study such as ferrite and pearlite. This model was capable of computing stress, strain, temperature and damage distributions. Figure 2.11 shows the accumulated damage during the FE simulation. The size of the grain was 10 μm.

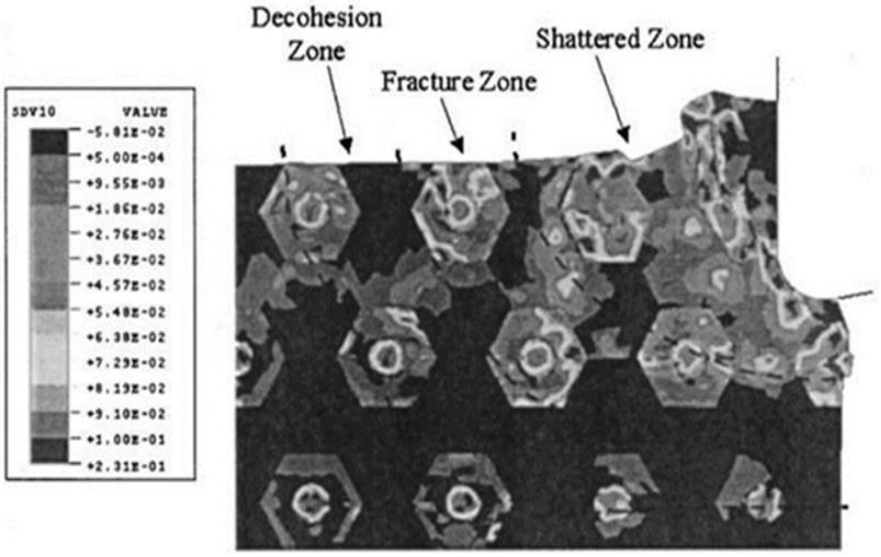

Figure 2.11: Machining iron using FEM [35]

Ghandehariun et al developed a novel analytical model to predict the cutting force required during the machining of MMCs. Orthogonal cutting was applied to Al 6061/Al_2O_3, Al 7075/Al_2O_3 particle reinforced MMCs with different volume fractures (10-20%) of Al_2O_3. This modeling showed good agreement with experimental data [36].

Ramesh et al. used dynamic finite element analysis to perform a systematic analysis of the mechanics of machining an Al6061/SiC MMC. They studied the possible encounters of the tool that included the tool facing SiC/matrix and tool ploughing SiC/matrix and considered the frictionless point contact between the tool and the work piece. This model was not able to describe the tool simultaneously interacting with SiC and the matrix [37].

Kishawy et al. proposed an energy-based analytical force model for orthogonal cutting of Al-MMCs [38]. In this model, the total specific energy for deformation had been estimated for the debonding of ceramic particles from the aluminum matrix as a function of the volume fraction and material properties. The model was validated and applicable for micro-sized ceramic reinforced MMCs in a turning configuration.

Fathipour et al. discussed the effective of cutting parameters on the machining forces of particle reinforced MMC. They found that change in the machining parameters results a change in the machining forces. The effect

of these parameters on the machining forces has been investigated in the machining of MMCs at three different percentages (fraction volumes 5%, 15% and 20%) of SiC reinforcement particles. The ABAQUS explicit software was used for the simulation in this study [39].

Ghandehariun et al addressed the challenges faced while machining MMCs with the development of novel modeling techniques as an understanding of the mechanics of the process was crucial. They used finite element modeling of the MMC machining process to facilitate an analysis of plastic deformations. A novel analytical model was used for the prediction of cutting forces while machining these composites. Transient Lagrangian modeling was used with adaptive remeshing control in order to reduce the effects of mesh distortions on an accurate estimation of plastic deformation while machining. A thorough understanding of MMC plastic deformations, which is achieved using the developed model, is an asset in the analysis of MMC behavior during the process [40].

Pramanik et al. used FE to model the tool-reinforcement particle interaction by considering three scenarios, namely with particles being on, above, and below the tool path (Figure 2.12). The evolution of stress and strain for the MMC and the effect of particle location on the tool wear were analyzed [41].

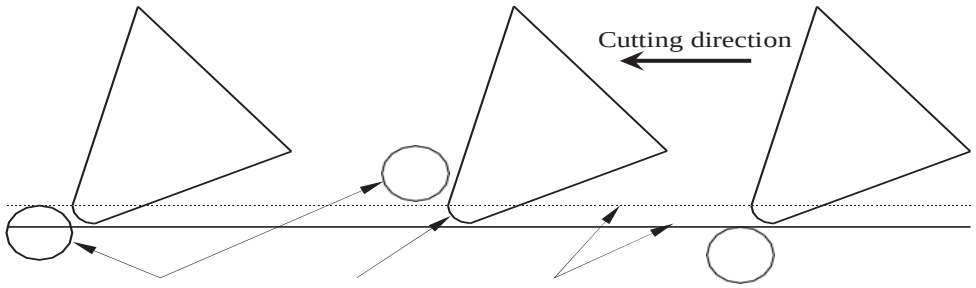

Figure 2.12: Particle locations: particles (a) along, (b) above, and (c) below the cutting path [41]

Liua et al., in their research, presented an orthogonal cutting simulation on the machining of 45% SiC/Al composites to develop an in-depth

understanding of surface defects in the micro milling of the SiC/Al2024 composites and their associated machining parameters. PCD micro end mill was used with a cutting tool of radius 5µm. The material removal mechanism and the surface defect formation were presented in three typical cases (Figure 2.13). The results revealed that surface defects are affected by the location of the tool-particle interaction and that the half interaction location might lead to the best surface quality [42].

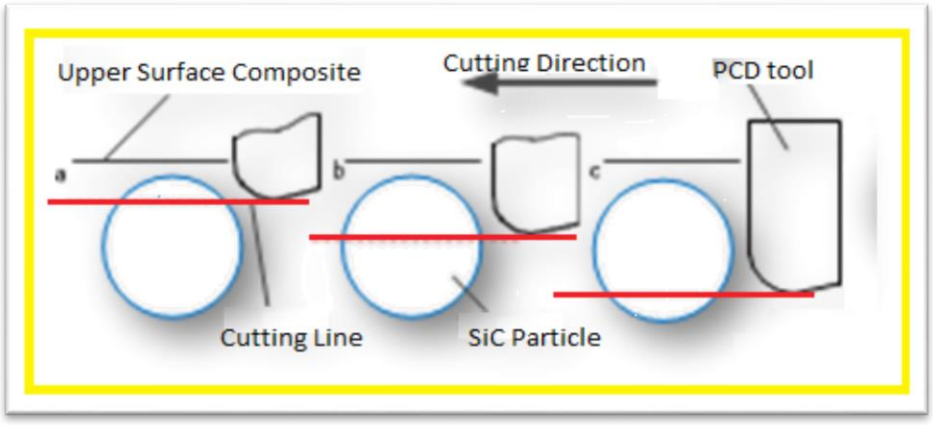

Figure 2.13: Interaction locations between the tool and particles [42] :

(a) The tool faces the upper SiC; (b) The tool faces the middle of the SiC; (c) The tool faces the under the SiC

Müller et al. studied the machining of SiC particle-reinforced aluminum matrix composites using electric discharge machining (EDM). It was found that the low electric conductivity of SiC particles led to a low material removal rate and high electrode wear, which mean increases in costs [43].

Another machining method is laser machining, which is used to make small diameter holes and for the cutting of MMCs. Results include poor surface quality as laser heating caused changes in the material microstructure [44].

Compared to the above methods, the mechanical machining process is promising for the mass production of MMC parts. This approach is also cost effective. The best type of cutting tool that is used for machining particulate MMCs is the poly crystalline diamond cutting tool. [45].

From the literature, we can see that with the development of modern computer technology, an FE simulation can be performed on more advanced solvers. FE solvers, such as *Abaqus*, are suitable for cutting simulations and they have become popular in academia.

Complex cutting geometries and material models can be embedded into the cutting process model.

Cutting MMCs is considerably difficult due to the extremely abrasive nature of the reinforcements that cause rapid tool wear and high machining costs. Thus, it is necessary to understand the effects of ceramic particles on the machining process.

The machining of P-Al-MMC needs further study in order to understand the behavior of this material.

CHAPTER 3

RESEARCH METHODOLOGY

3.1 Research Motivation

Our motivation is to provide a clear understanding of the actual behavior of the particulate aluminum metal matrix composite during the

cutting process and to find the cutting force required with stress while machining this type of material.

3.2 Approach

The background and literature review of previously published work on machining operations of MMCs was presented in Chapter 2.

In this thesis, using finite element modeling, four models were built to simulate the cutting process, namely orthogonal cutting. The FEM prediction is compared with experimental data from the literature review.

The first model was Model I where a simulation of machining aluminum alloy 6061 with and without damage was modeled. The results were compared with experimental results for different cutting conditions. The last step in this model evaluated the effect of the rake angle, clearance angle and friction models on the output.

The three models are used to simulate the machining of p-Al-MMCs. The selected matrix material was aluminum alloy A359 reinforced with silicon carbide (SiC) particles having a diameter of 20 μm with a volume fraction of 20%. The type of material, reinforced particle, size of particle, and volume fraction were used depend on the same type of particle reinforced aluminum MMC that available in literature review. The accuracy of three different modeling approaches to predict the machining force was studied. In the first approach, p-Al-MMC was modeled using equivalent homogeneous material (EHM) model where plastic deformation and damage evolution are governed by high-strain rate deformation behavior of a A359/SiC/20p composites and Johnson-Cook damage models, respectively.

The second and third approaches attempted to model p-Al-MMCs as a two-phase heterogeneous material, where it is assumed that the matrix consists of a periodic array of non-agglomerated particles of identical size, shape and distance. The second approach was Model III, this model simulates the machining of particulate MMCs as heterogenous material with a periodic square distribution. The interface between particles and the matrix was defined.

The third approach, Model IV, focused on simulation of machining particulate MMCs as heterogenous material but with periodic hexagonal particle distribution.

The results of three models validated were compared with the experimental results. The FEM was able to provide an understanding the matrix/particles interaction with the cutting tool. The FE can also provide a clear image about plastic deformation, chip removal and the important point on how much cutting force is required while cutting.

3.3 Methodology

The two-dimensional FEM is built to machine particulate MMC. These models are created using Abaqus/Explicit commercial FEM software to simulate the cutting process.

Abaqus is an FE analysis program that can be used for a variety of problems such as metal cutting. Abaqus does not have a module for specific forming processes. Therefore, the user has to define the tool and work piece geometries, cutting conditions, the solver technique, boundary conditions and mesh size. This program does not have a material library, but it does allow the user to configure materials using a variety of models. The significant advantage of using this software is in modelling systems in a high level of detail. The type of data is based on the Explicit Model.

A simulation will contain three parts: a matrix, particles which are used to create the work piece material and the cutting tool. The type of cutting tool is an analytical rigid body. Analytical rigid surfaces are geometric surfaces with profiles that can be described with straight and curved line segments.

An analytical rigid surface does not contribute to the rigid body's mass or inertia properties.

Analytical rigid surfaces are always single-sided with their orientation specified through their definition. Therefore, contact interaction is recognized only on the outer boundary of an analytical rigid surface. Many curved geometries can be modeled exactly with analytical rigid surfaces because of the ability to parameterize the surface with curved line segments. The result is a smoother surface description, which can reduce contact noise and provide a better approximation to the physical contact constraint.

The interaction between a particle and a matrix is defined and the interaction of both the matrix and the particle with the cutting tool is defined. A Coulomb friction model is used based on the results of friction coefficient.

A tie constraint is applied between the particle and the matrix. The contact type is a surface to surface contact.

The size of the mesh selected for the work piece is divided into two regions with a parting line. The cutting area is a very fine mesh and the second a coarse mesh. The type of mesh is free.

The results of the FEM are compared and validated with experimental data.

These models were developed for the prediction of the cutting force required while machining. The cutting force is very important to study many parameters such as the effect of the cutting tool type or geometry, cutting conditions, distribution of particles periodic square or the periodic hexagonal, on the machining.

The failure parameter for model III and model IV depending on Johnson-Cook plasticity with Johnson-Cook damage. The failure model for all simulations depends on damage parameter D. The damage parameter is the ratio between the increment of equivalent plastic strain to the equivalent strain at failure, which means that the element assumed to fail will be deleted when D exceeds unity.

These three models for machining particulate MMCs will be used in order to develop a constitutive model which introduces a better description of particulate MMC behavior while being machined.

The basic specifications of the system used to perform the simulation is as follows:

Processor: Intel (R) Xeon (R) CPU E5-2640 V3 2.60 GHz
Installed Memory (RAM): 32.0GB
System type: 64-bit operating system
Windows type: Windows 7 Professional.

3.4 Material Constitutive Models

In order to be successful, a material constitutive model needs to be reliable and mathematically simple. Some are simple models while others require many material constants. Determining these constants is quite complicated and requires a large number of experiments. The difficulty in recreating the same conditions of machining operations can lead to modelling limitations. Selecting the correct equations to describe material behavior is a crucial part of setting up a solid mechanics analysis. An incorrect model used or the inaccurate material properties will lead to completely invalid predictions. It has been stated already that the constitutive model for a material is a set of equations relating stress to strain (and possibly strain history, strain rate and other field quantities). In the following subsections, several flow stress relations are presented.

3.4.2 Power Law Flow Stress Model

This constitutive model assumes a flow stress as a function of strain, strain rate and temperature [46].

$$\bar{\sigma} = \sigma_0 \left(\frac{\bar{\varepsilon}}{\bar{\varepsilon}_0} \right)^n \left(\frac{\dot{\bar{\varepsilon}}}{\dot{\bar{\varepsilon}}_0} \right)^m \left(\frac{T}{T_0} \right)^\tau \quad \text{..... (1)}$$

3.4.2 Oxley's Constitutive Flow Stress Model

This constitutive model expresses a flow stress as a work-hardening where σ_0 is the strength coefficient and n is the strain hardening coefficient behavior (Eq. 2) [47].

$$\bar{\sigma} = \sigma_0 \bar{\varepsilon}^n \quad \text{..... (2)}$$

3.4.3 Strain-Path Dependent Flow Stress Model

The flow stress model captures the effect of loading history as well as the coupling effect of the strain rate and temperature. *K* and *m* are constants and *A*, *M*, *N* are functions of the temperature [48], as shown in Eq. 3.

$$\bar{\sigma} = A(10^{-3}\dot{\bar{\varepsilon}})^M e^{KT}\left[\int_{T,\bar{\varepsilon}=\dot{\bar{\varepsilon}}} e^{\frac{-KT}{N}} (10^{-3}\dot{\bar{\varepsilon}})^{-m/N} d\bar{\varepsilon}\right]^N \quad \text{..... (3)}$$

The model is considered unique to recover the historical effects of strain and temperature during metal cutting.

3.4.4 Johnson-Cook (J-C) Flow Stress Model

The flow stress is assumed to be a function of strain, strain rate and temperature effects. This is verified using a wide range of strain rates as well as dynamic Hopkinson bar tensile tests and Hopkinson bar tests at elevated temperatures [49].

$$\bar{\sigma} = \left[A + B(\bar{\varepsilon})^n\right]\left[1 + C\ln(\frac{\dot{\bar{\varepsilon}}}{\dot{\bar{\varepsilon}}_\circ})\right]\left[1 - \left(\frac{T - T_{room}}{T_{melt} - T_{room}}\right)^m\right] \quad \text{..... (4)}$$

The equivalent plastic stress $\bar{\sigma}$ is a function of strain $\bar{\varepsilon}$,strain rate$\dot{\bar{\varepsilon}}$, and temperature (T) .A,B,C and m are the constant previously determined based on flow stress data obtained from the static tensile and torsion tests as well as mechanical test .Hardening strain exponent (n). T_{room} is the room

temperature while T_{melt} ,is the melting point temperature of the work piece material.

3.5 Damage Models

Metal cutting involves material fracture. Chip separation relates to the material failure criterion that allows chip separation from the work piece. There are many types of failure model, but only failure models used in the cutting process as found in literature will be mentioned.

3.5.1 Johnson and Cook Failure Model

This approach is widely used to model the ductile failure of materials experiencing high pressures, strain rates and temperatures. It consists of three independent terms that define the dynamic fracture strain: the first term relates to pressure dependence, the second to strain-rate dependence and the third to the temperature [50].

$$\varepsilon_f = \left[d_1 + d_2 \exp\left(d_3 \frac{\sigma_m}{\sigma} \right) \right] \left[1 + d_4 \ln \frac{\dot{\bar{\varepsilon}}}{\dot{\bar{\varepsilon}}_0} \right] \left[1 + d_5 \left(\frac{T - T_{room}}{T_m - T_{room}} \right) \right] \quad \text{..... (5)}$$

The constants d_1 to d_5 represent the material parameters of the damage law and are obtained from tensile tests, σ_m represents the hydrostatic stress and σ the von Mises equivalent stress. The damage in a given finite element is defined as:

$$D = \sum \frac{\Delta \varepsilon}{\varepsilon_f} \quad \text{..... (6)}$$

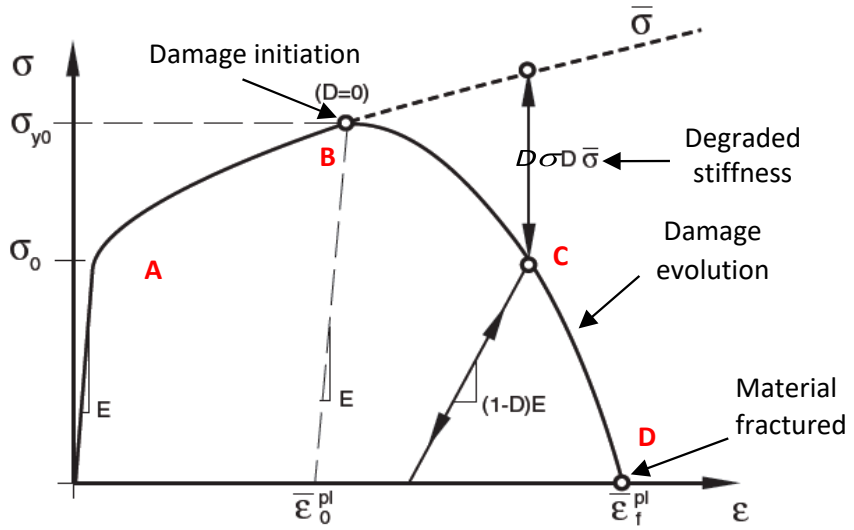

Figure 3.1: Stress-stain curve: progressive damage degradation [51]

3.5.2 Wilkins Failure Model

This model considers the hydrostatic pressure effect on damage accumulation. The equation of effective plastic strain weighted by w_1, w_2 is:

$$D = \int_0^{\bar{\varepsilon}_f} w_1 w_2 d\bar{\varepsilon} \quad \text{..... (7)}$$

where D is the damage indicator weighting terms [52]. This model is not popularly used in machining processes.

3.5.3 Modification of the Cockcroft-Latham Failure Model

The Cockcroft-Latham failure model was applied in forming processes and machining processes. The damage is equal to the integral of the maximum principle stress σ_1 to the effective plastic stress $\bar{\sigma}$ (Eq. 8) [53].

$$D = \int_0^{\bar{\varepsilon}_f} \frac{\sigma_1}{\bar{\sigma}} d\bar{\varepsilon} \quad \text{..... (8)}$$

3.5.4 Bao and Wierzbicki Model

Bao and Wierzbicki proposed an empirical fracture model depending on stress triaxiality. They found that ductile material would fail if stress triaxiality was higher than –⅓. Where σ_H is hardening stress and $\bar{\sigma}$ is Von Mises stress. They also found that the fracture locus would exhibit three branches in the whole range of stress triaxiality as a result of two failure mechanisms, including void growth and "shear decohesion" (as seen in Figure 3.1). The mathematical expressions of the three branches in the empirical B-W fracture model are given as [54]:

$$\bar{\varepsilon}_f = \begin{cases} 0.1225\left(\frac{\sigma_H}{\bar{\sigma}} + \frac{1}{3}\right)^{-0.46}, -\frac{1}{3} < \left(\frac{\sigma_H}{\bar{\sigma}}\right) \le 0 \\ 1.9\left(\frac{\sigma_H}{\bar{\sigma}}\right)^2 - 0.18\left(\frac{\sigma_H}{\bar{\sigma}}\right) + 0.21, 0 < \left(\frac{\sigma_H}{\bar{\sigma}}\right) \le 0.4 \\ 0.15\left(\frac{\sigma_H}{\bar{\sigma}}\right)^{-1}, 0.4 < \left(\frac{\sigma_H}{\bar{\sigma}}\right) \le 0.95 \end{cases} \quad \text{.....} \quad (9)$$

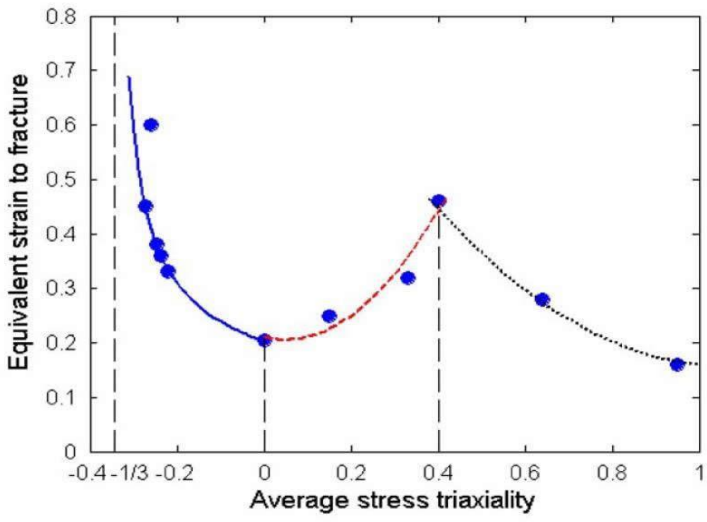

Figure 3.2: Fracture locus of the empirical B-W model [55]

CHAPTER 4

4. FINITE ELEMENT METHOD METAL CUTTING SIMULATION OF HOMOGENOUS MATERIAL

Metal cutting researchers focus on determining the best cutting conditions and tool geometries for process efficiency. Experimental works are needed to obtain results, but they are expensive and time consuming. In addition, simplified analytical methods have limited applications and they cannot be used for complex cutting processes. At this point, the finite element method has been most frequently used in metal cutting analysis. Various outputs and characteristics of metal cutting processes, such as cutting forces, stresses, temperatures, chip shape, etc., can be predicted using FE without any experimentation.

Today simulation is an essential tool regarding product quality, cost reduction and the overall prediction of metal cutting operations, contributing to a reduction or even elimination of trial and error approaches. Figure 4.1 shows the growth rate of published articles on machining simulations and machining modeling in the 1970-2015 period [56].

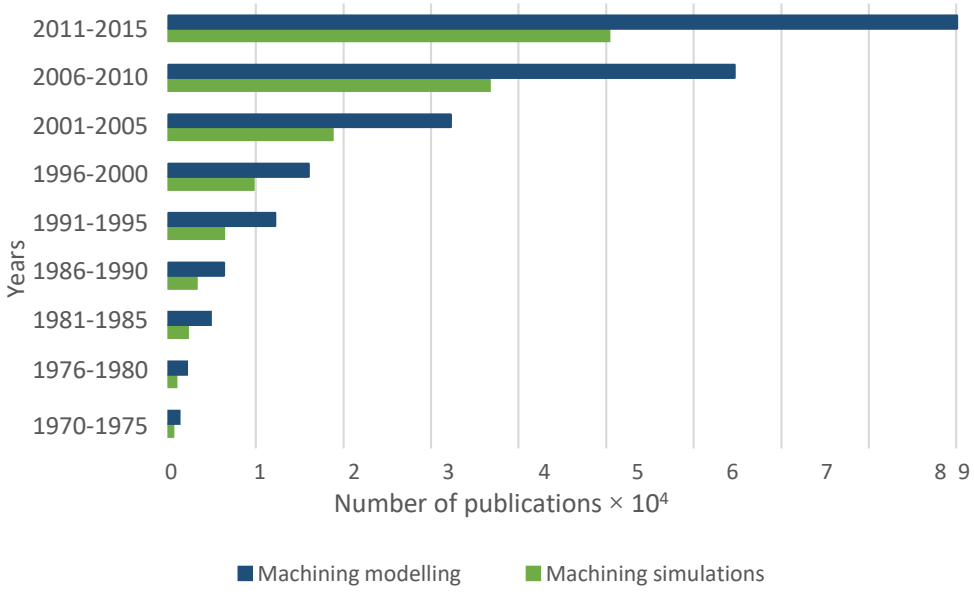

Figure 4.1: Number of machining simulations and modelling articles published in the 1970-2015 period [56]

4.1 Model I

Finite Element Modeling is used for machining aluminum alloy 6061. A 2D model was built to simulate the turning operation with the same cutting parameters used in the experiment [57].

4.1.1 Work piece material and cutting tool geometry

The work piece material used is aluminum alloy 6061, which is a precipitation hardening alloy containing magnesium and silicon as its major alloying elements.

It was developed in 1935 and originally called Alloy 61S. It has good mechanical properties and exhibits good weldability. It is one of the most common alloys for general purpose use.

The chemical composition (wt., %) of this alloy are shown in Table 4.1.

Table 4.1: The chemical composition (wt., %) of aluminum alloy 6061 [58]

Al alloy	Si	Fe	Cu	Mn	Mg	Cr	Zn	Ti	Others Each	Others Total	Al
6061	0.40 -0.8	0.7	0.15-0.40	0.15	0.8-1.2	0.04-0.35	0.25	0.15	0.05	0.15	Remain -der

Work piece geometry

The work piece geometry used for 2D simulation is a rectangle of X × Y as seen in figure 4.2.

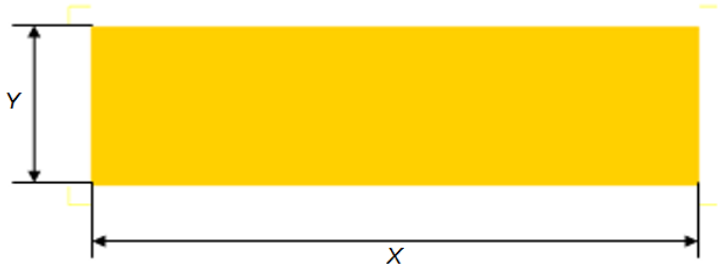

Figure 4.2: Work piece geometry for 2D simulation

Tool material and geometry

The cutting tool operated under extreme pressure and temperature conditions during use. Materials for cutting tools require appropriate properties to resist plastic deformation, fractures, abrasion, chemical attack and wear and they must maintain a sharp edge for a long period of time. Hot

hardness is the most basic requirement of a tool material. The cutting tool properties used in experiment are presented in Table 4.2 [57].

Table 4.2: Mechanical and physical properties of tungsten carbide cutting tool

Material	Density ($kg.m^{-3}$)	T. Conductivity ($W.m^{-1}.^oC^{-1}$)	Vol. heat capacity ($MJ.m\text{-}3.^oC^{-1}$)	Thermal expansion coefficient ($\times 10^{-6}\ K^{-1}$)	Elasticity M. (GPa)	Poisson ratio
WC	15000	100	15	5.0	650	0.25

The cutting tool used in the simulation was assumed to be a rigid body with a normal rake angle of 0° and a normal clearance angle of 7°. The cutting tool radius is 20 μm.

4.1.2 Work Material Constitutive Models

One of the most important subjects in metal cutting simulation is the proper modelling of the flow stress of the work piece material in order to obtain authentic results. Flow stress is an instantaneous yield stress that depends on strain, strain rate and temperature. These parameters are represented in the mathematical forms of constitutive equations.

Johnson and Cook (1993) developed a material model based on torsion and the dynamic Hopkinson bar test over a wide range of strain rates and temperatures.

This constitutive equation was established as follows, (Eq.4, chapter 3):

$$\bar{\sigma} = \left[A + B(\bar{\varepsilon})^n \right] \left[1 + C \ln\left(\frac{\dot{\bar{\varepsilon}}}{\dot{\bar{\varepsilon}}_\circ}\right) \right] \left[1 - \left(\frac{T - T_{room}}{T_{melt} - T_{room}} \right)^m \right]$$

The first parenthesis is the elastic-plastic term representing the strain hardening. The second is the viscosity term that shows that the flow stress of the material increases when the material is exposed to high strain rates. The last is the temperature softening term. *A*, *B*, *C* and *m* are the material constants that are found through material tests available in. *T* is the instantaneous temperature, $Troom$ is the room temperature and T_{melt} is the melting temperature of a given material. The Johnson-Cook material model assumes that the flow stress is affected by strain, strain rate and temperature

independently. The constants for the Johnson-Cook constitutive model for aluminum alloy 6061 are shown in Table 4.3.

Table 4.3: Constants for Johnson-Cook constitutive model for Aluminum alloy 6061 [59]

***A* [MPa]**	***B* [MPa]**	***C* (-)**	***n* (-)**	***m* (-)**	T_{melt} **(K)**
270	154.3	0.002	0.289	1.43	947

Johnson-Cook Damage

In order to simulate the separation between the chip and the work piece, a dynamic failure model was used for the Johnson-Cook model in *Abaqus*/*Explicit*. The Johnson-Cook dynamic failure model is based on the value of the equivalent plastic strain at element integration points. The failure is assumed to occur when the damage parameter *D* exceeds 1. This is a physical criterion. The damage parameter *D* (Eq.6, chapter 3) is defined as follows:

$$D = \sum \frac{\Delta \varepsilon}{\varepsilon_f}$$

The Johnson-Cook damage equation(Eq.5,chapter 3) is:

$$\varepsilon_f = \left[d_1 + d_2 \exp\left(d_3 \frac{\sigma_m}{\sigma} \right) \right] \left[1 + d_4 \ln \frac{\dot{\bar{\varepsilon}}}{\dot{\varepsilon}_0} \right] \left[1 + d_5 \left(\frac{T - T_{room}}{T_f - T_{room}} \right) \right]$$

where d_1 to d_5 are the failure parameters for the Johnson-Cook Damage. The failure parameters for aluminum alloy 6061, are presented in the table below [60].

Table 4.4: Johnson-Cook damage criteria for aluminum alloy 6061 [60]

d_1	d_2	d_3	d_4	d_5
–0.77	1.45	–0.47	0.0	1.60

4.1.3 Meshing

A continuous region is divided into discrete regions called elements in FE analysis. This procedure is called discretization or meshing. An initially designed FE mesh cannot hold its original shape and it is distorted due to severe plastic deformation during metal cutting or metal forming

processes. Distortion causes convergence rate errors and numerical errors. To solve with this problem, a new FE mesh must be generated by changing the size and distribution of the mesh (Figure 4.3).

After modelling the metal cutting components individually, the next step is to assemble them due to the cutting conditions. Another important step is to define the contact between the work piece and the tool. The tool is selected as the master object because it is defined as a rigid object. The work piece is defined as slave object.

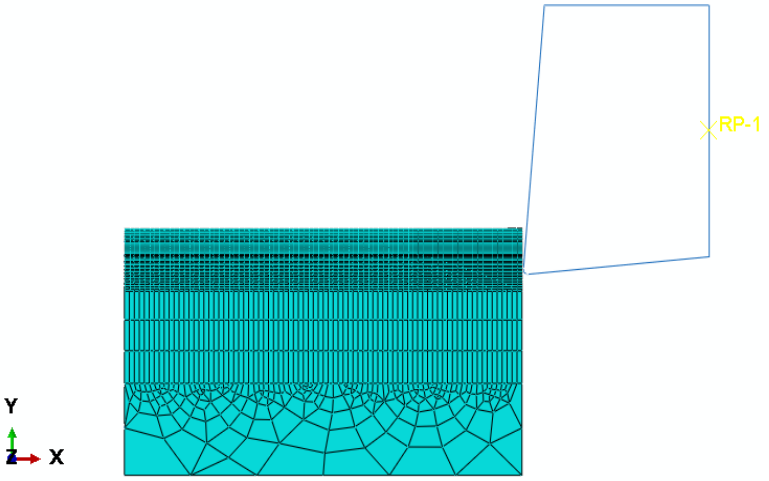

Figure 4.3: The size and distribution of the mesh

4.1.4 Cutting conditions

The cutting speed ranged from 300 to 500 m/min. The feed was 0.12 and 0.15 mm/rev. uncut chip thickness 1 mm and the cutting width was 4 mm. Figure 4.4 shows simulation results of machining with Johnson-Cook model.

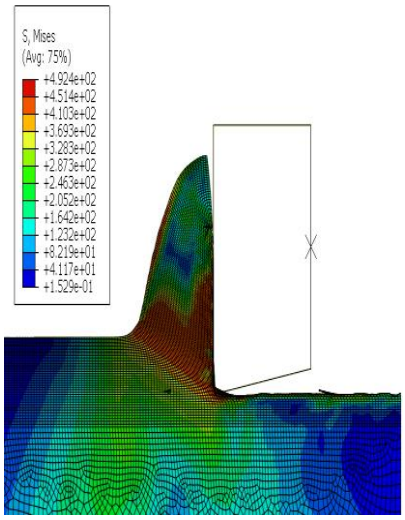

Uncut chip thickness 0.12 mm, cutting speed 300m/min.

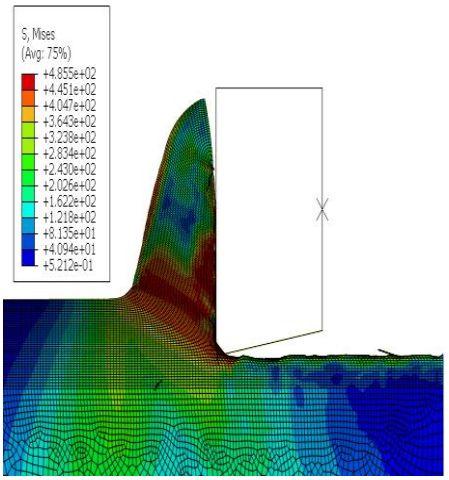

Uncut chip thickness 0.15 mm, cutting speed 300m/min.

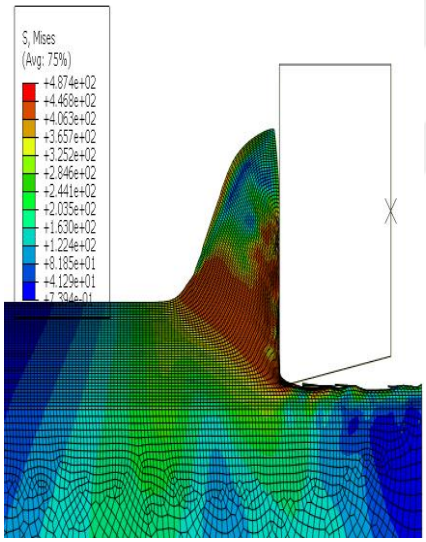

Uncut chip thickness 0.12 mm, cutting speed 500m/min.

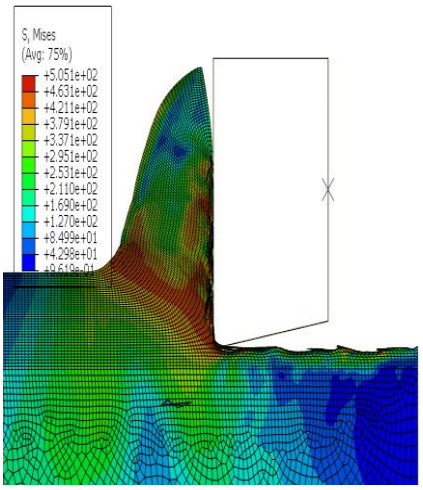

Uncut chip thickness 0.15 mm, cutting speed 500m/min.

Figure 4.4: Finite Element Modeling of Machining Aluminum alloy 6061 with maximum stress (MPa) during machining.

FEM is also used to simulate the machining of aluminum alloy with Johnson cook plasticity table 4.3 and without Johnson-Cook damage, the cutting force is V = 500 m/min and uncut chip thickness is 0.15 mm as shown in figure 4.5.

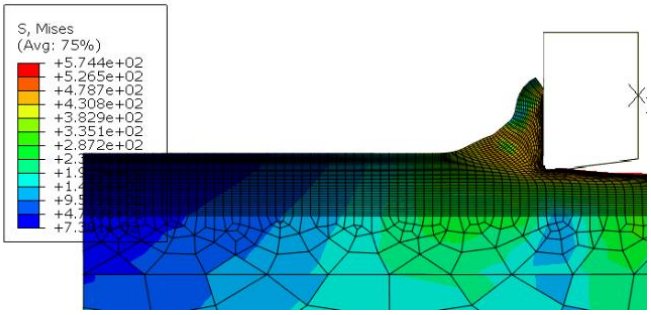

Figure 4.5: Finite Element Modeling for machining aluminum alloy 6061with maximum stress while machining (without J-C damage)

Results

The cutting force values predicted for the machining of aluminum alloy 6061 with the FE model with J-C damage is compared with experimental values under different cutting conditions (table 4.5). The cutting forces increase with the increase of uncut chip thickness at the same cutting speed. The cutting forces increase with the increase of cutting speed with a certain range. The cutting forces start to decrease due to the thermal softening when the cutting speed increase from 300m/min to 500 m/min at the same uncut chip thickness. The reason is that at low speed, heat generation is relatively low, thus the increase of cutting forces is likely attributed to the increased strain rate. However, when cutting speed exceeds a certain value, heat generated by machining can lead to the thermal softening of workpiece. The close agreement between the results verifies the ability of the model to provide accurate estimations of the cutting force.

Table 4.5: Results of the cutting force for FE simulation with J-C damage for aluminum alloy 6061

Cutting Condition		**V = 300m/min** a_c **= 0.12 mm**	**V = 300m/min** a_c **= 0.15 mm**	**V = 500m/min** a_c **= 0.12 mm)**	**V = 500m/min** a_c **= 0.15 mm**
Experimental	F_c **(N)**	87.5	115	85	107.5
FEM Simulation with J-C damage	F_c **(N)**	85.7	104	84.7	98
Relative error F_c		2%	9.5%	0.3%	8.8%

The cutting force average result (*N*) for aluminum alloy 6061 without J-C Damage is found. From this simulation, the cutting force prediction is an over estimation in comparison to the experimental values under different cutting conditions. This means that the FE model without J-Damage is unable to provide a good estimation of the cutting force.

4.1.5 Effect of Rake Angle on Machining Force

The normal rake angle (α) is a parameter used in various cutting and machining processes, describing the angle of the cutting face relative to the workpiece. This angle takes negative, zero and positive values. For ductile materials, a positive rake angle is used, while for high strength materials negative rake angles are used. Three simulations of machining aluminum alloy 6061 are built under the same cutting conditions (v = 500 m/min and uncut chip thickness = 0.12 mm) with α = 10°, 0° and −10° to find the effect of the rake angle on the cutting force, as shown in Figure 4.6.

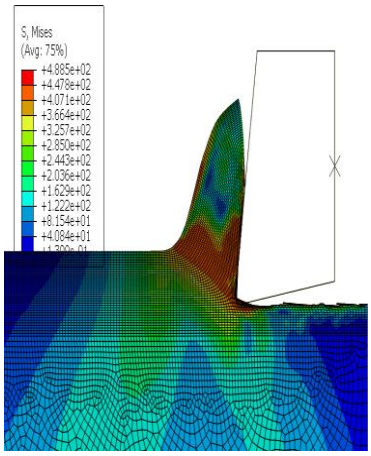

α=10°, V = 500m/min, a_c = 0.12 mm

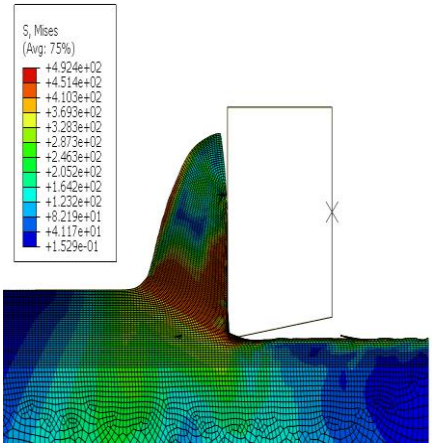

α=0°, V = 500m/min, a_c = 0.12mm

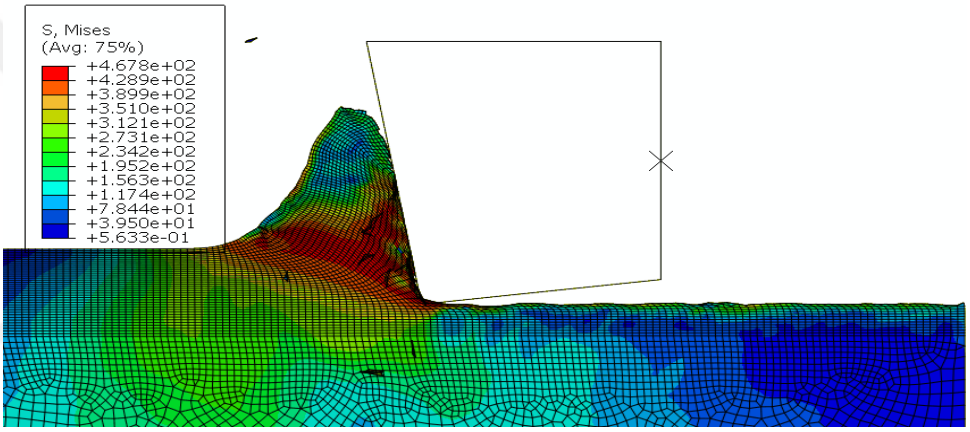

α = –10°, V = 500m/min, a_c = 0.12 mm

Figure 4.6: FEM of machining aluminum alloy with different rake angle values and maximum stress while machining

Results

Average cutting forces in the FE simulation results show that the cutting forces decrease with an increase in the rake angle, as shown in Figure 4.7.

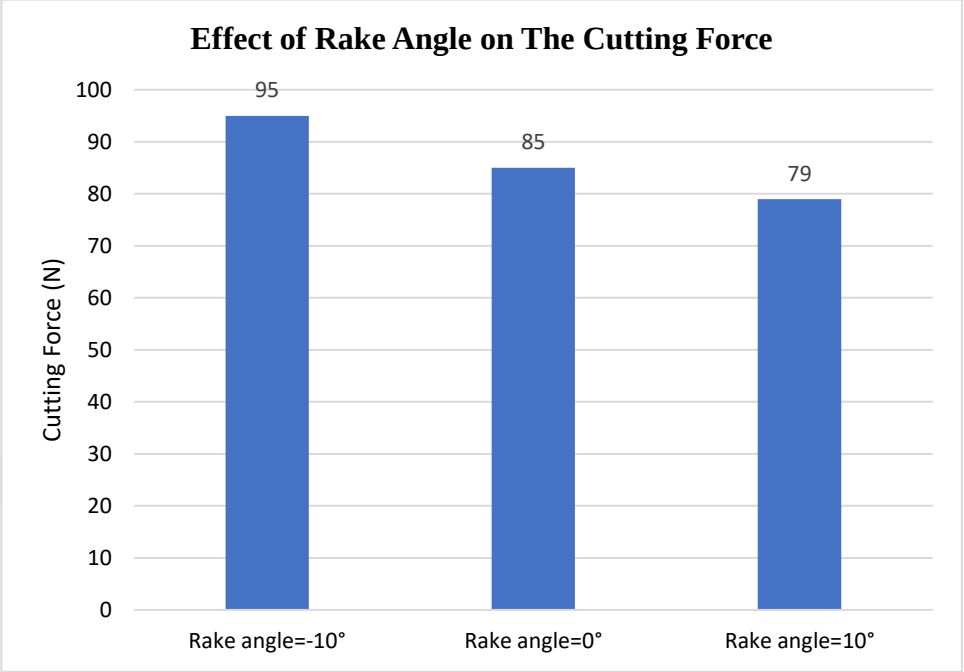

Figure 4.7: Effect of rake angle on machining force

4.1.6 Effect of Clearance Angle on Machining Force

Clearance angle is a small clearance between the tool flank and the transient cut surface, which helps to protect the flank from abrasion. Three values (4°, 8°, 16°) of clearance angle were modeled (see Figure 4.8) under the same cutting conditions (v = 500 m/min and uncut chip thickness = 0.12 mm) to find its effect on the cutting force.

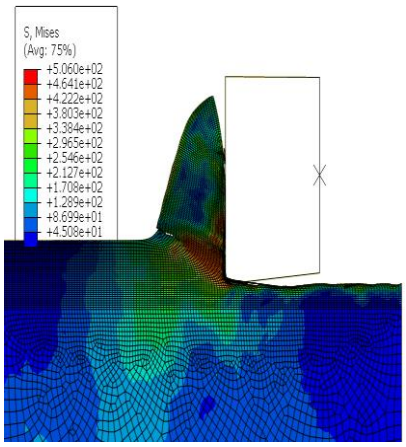

Clearance angle = 4°

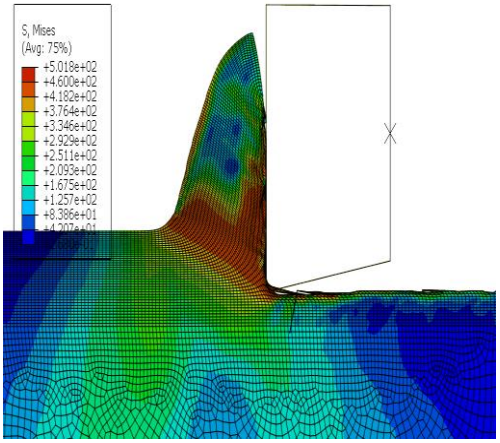

Clearance angle = 8°

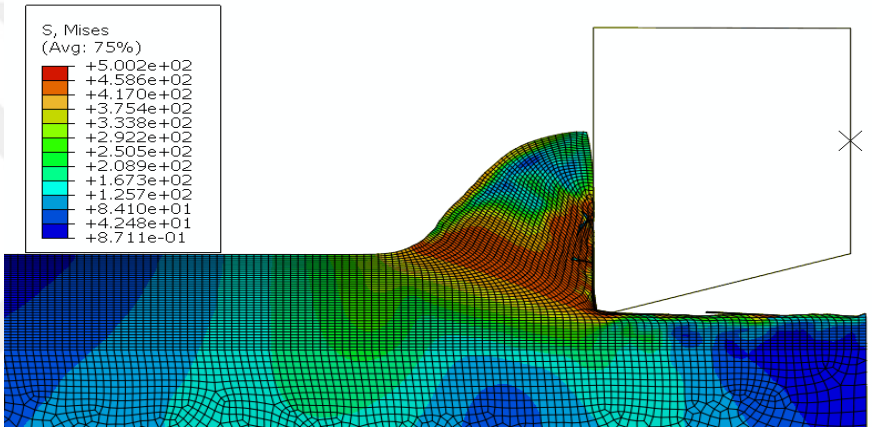

Clearance angle = 16°

Figure 4.8: Different clearance angles at maximum stress during machining

Results

An increase in the clearance angle causes a decrease in the cutting force during the machining operation, as shown in Figure 4.9.

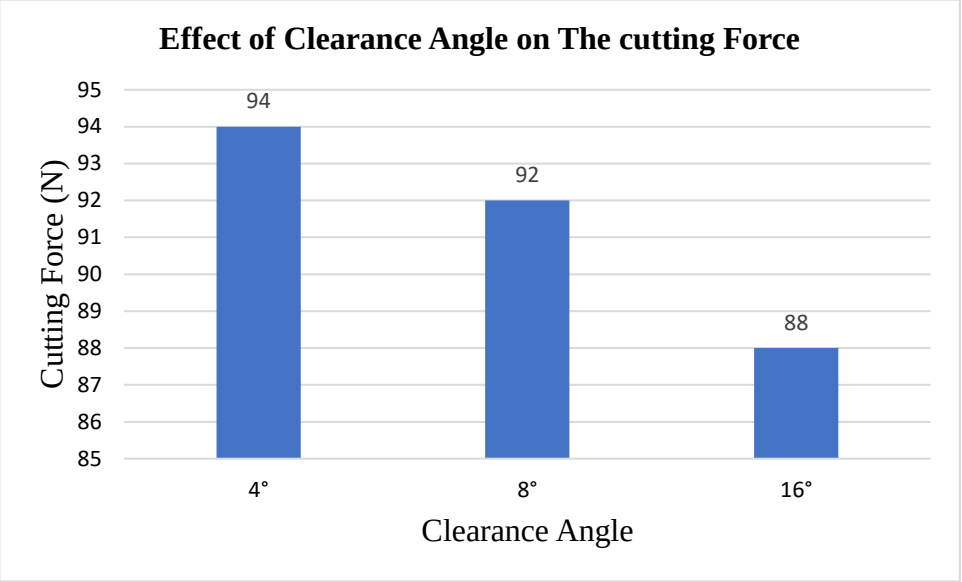

Figure 4.9: Effect of changing the clearance angle on the cutting force

4.1.7 Effect of the friction coefficient on the cutting force

To find the effect of the friction coefficient on the cutting force, six simulations were built with different friction coefficients (0.2,0.15,0.17, 0.4, 0.6, 0.8) and fixed cutting conditions. The average cutting force was compared with the experimental data (v = 500 m/min and uncut chip thickness = 0.12 mm) where F_c = 85 N to find the error figure (4.10).

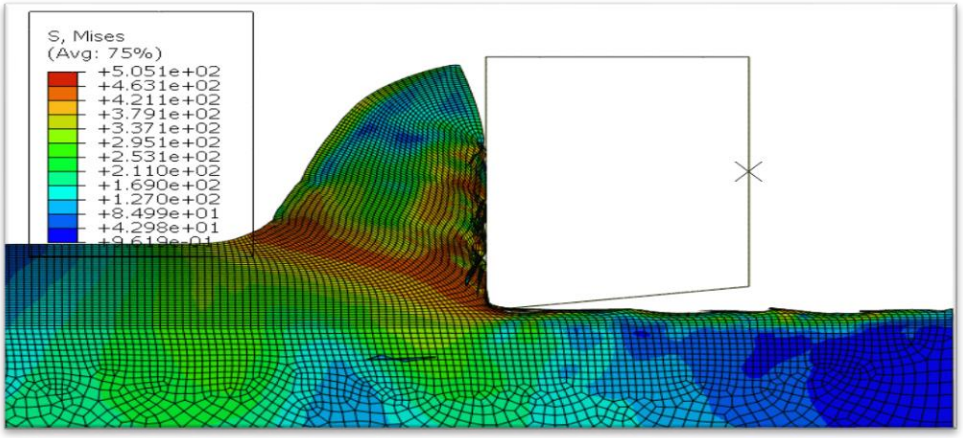

(a) Friction coefficient = 0.15 with v = 500 m/min, uncut chip thickness = 0.12 mm

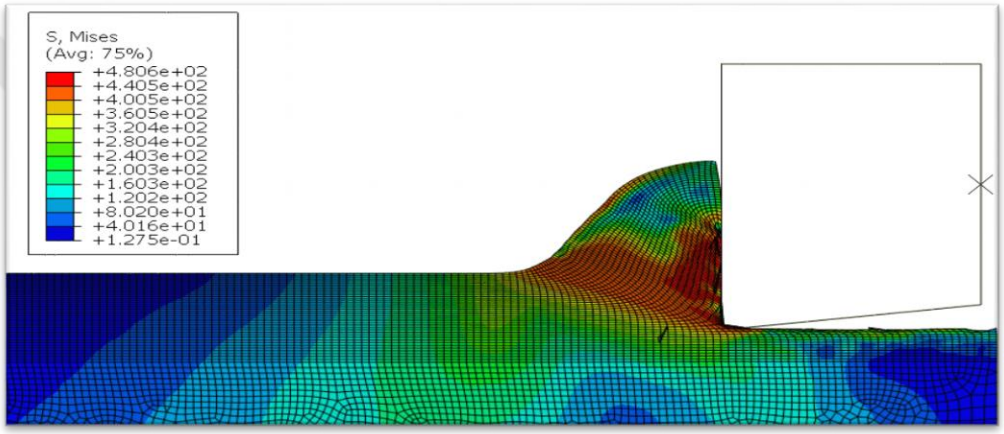

(b) Friction coefficient = 0.17 with v = 500 m/min, uncut chip thickness = 0.12 mm

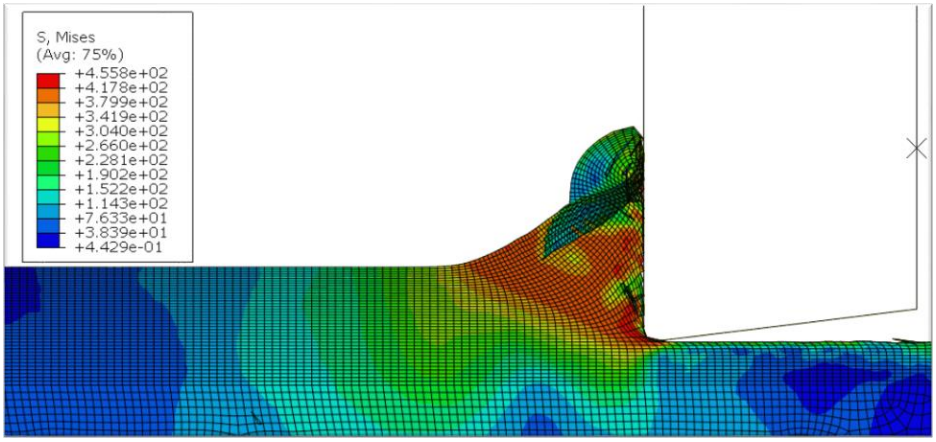

(c) Friction coefficient = 0.8 with v = 500 m/min, uncut chip thickness = 0.12 mm

Figure 4.10: Effect of friction coefficient on stress distribution (MPa)

Results

An increase of the friction coefficient causes an increase in the cutting forces.

Table 4.6: Effect of friction coefficient on cutting force

Friction coefficient	0.1	0.15	0.17	0.2	0.4	0.6	0.8
Fc (N)	82	83.2	84.7	88.2	89	89.3	92
Error%	3.5%	2.1%	0.35%	–3.8%	–4.7%	–5%	–8%

4.2 FINITE ELEMENT MODILING OF MACHINING PARTICLE RINFORCED ALUMINUMMETAL MATRIX COMPOSITES

Finite element modeling of machining particles MMC is more difficult compared with machining homogeneous materials. These difficulties include mesh distortion and the interface between particle, matrix and particle/matrix with the cutting tool. Therefore, many strategies are used to describe the behavior of particle reinforced metal matrix composites (PRMMCs) during a machining process. In this study, the accuracy of three different modeling strategies to predict machining forces of particulate aluminum metal matrix composites (p-Al-MMC) have been studied. The type of material is aluminum alloy A359 (table 4.7) reinforced with SiC particles with a diameter of 20 μm and a volume fraction of 20%.

In the first approach, the p-Al-MMC is modeled as homogeneous material.

The reinforcement particles and the matrix are modeled as a heterogeneous material for the second and the third models. In the heterogeneous models, two approaches are used depending on the particle distribution in the matrix. The first approach is a periodic square particle distribution, while the second approach depends on a periodic hexagonal particle distribution.

The three models, Model II, Model III and Model IV, are used to describe the behavior of p-Al-MMC during the machining process in comparison with experimental data [61] under the same cutting conditions and tool geometries as shown in table 4.9 and 10, respectively with the same coefficient of friction is 0.48 [61].

Table 4.7: A359/SiC/20p chemical composition (wt., %) [62].

Element	Si	Fe	Cu	Mn	Mg	Zn	Ti	Al
%	8.5-9.5	0.2	0.2	0.1	0.50-0.70	0.1	0.2	89-91

Table 4.8: Work piece and cutting tool properties

Materials	Aluminum alloy A359 matrix	Reinforcement (SiC) particles	Cutting Tool type (PCD)
Density (kg/m^3)	2700	4370	3500
Young's modulus (MPa)	72000	408000	800000

Table 4.9: Cutting conditions of MMCs

Cutting speed	300 m/min
Feed rate	0.1 mm/rev
Uncut chip thickness	1 mm

Table 4.10: Cutting tool geometry

Rake angle	Clearance angle	Edge radius
5°	5°	20 μm

4.2.1 Model II

Equivalent homogenous material (EHM)

The constitutive equation chosen to model the EHM material properties is based on the work of Li et al. who studied high-strain rate deformation behavior of a A359/SiC/20p composites [63,64]. The study was directed towards understanding the behavior of these composites under impact loading for ballistic applications. The proposed constitutive equation is given in Eq. 10 and 11. The temperature dependency model in Eq. 10 is added to the constitutive based on the experimental tests carried out by Miguelez and Navarro on a A359/ SiC/20p composite. Table 4.11 summarizes the values of the material constants and other material parameters necessary for modeling [65,66].

$$\sigma(V_f,\varepsilon,\dot{\varepsilon},\mathrm{T}) = \sigma_o(\varepsilon)\, g(V_f)\left(1+\left(\frac{\dot{\varepsilon}}{\dot{\varepsilon}_o}\right)^{0.45}\right)\left(1+\left(\frac{\dot{\varepsilon}}{\dot{\varepsilon}_o}\right)^{0.45} V_f\right)\left[1-\left(\frac{T-T_r}{T_m-T_r}\right)\right]^{5.5} \quad (10)$$

$$g(V_f) = 1+1.17V_f + 2.28V_f^2 + 21.0V_f^3 \ldots\ldots\ldots\ldots\ldots\ldots\ldots \quad (11)$$

Where σ is the overall flow stress, vf the particle volume fraction, ε the overall strain_ $\dot{\varepsilon}$ the Overall strain rate, T the temperature, $\sigma_o(\varepsilon)$ the stress–strain response of the matrix at quasi-static rates of deformation, vf the volume fraction and g(vf) is the strengthening function dependent on the volume fraction.

Table 4.11: The values of the material constants

Rate sensitivity parameters	**Tr Reference temperature** °C	**Tm Melting point** °C	**E Youngs modulus** GPa	**V Poisons ratio**	**Yield strength** MPa	**Density** gm/cm³
1.47* $10^5 S^{-1}$	23	615	98.6	0.26	260	2.77

The relationship between flow stress and true strain at various strain rates used in the simulation is shown in figure 4.11.

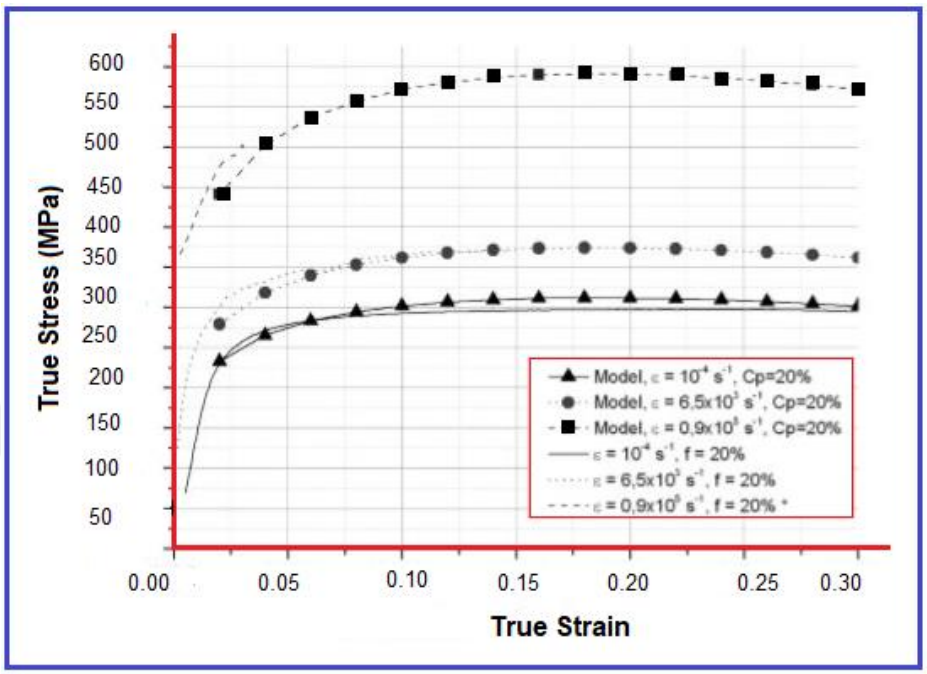

Figure 4.11: Comparison of experimental and prediction data of A359/ SiC/20p composite at various strain rate [66].

The chip separation in the chip is simulated using the Johnson and Cook damage which takes in to account strain, strain rate, temperature and pressure.Eq.5 chapter 3. Parameters for the Johnson and Cook damage law table 4.12.

Table 4.12: Parameters for the Johnson and Cook damage law

JC damage parameters	d_1	d_2	d_3	d_4	d_5
	0.071	1.248	−1.142	0.147	0.1

The cutting condition and cutting tool geometry as shown in table 4.9 and 10, respectively.

Figure 4.12 is shows the Mises Stress distribution obtained from machining simulation of EHM for p-Al-MMC model.

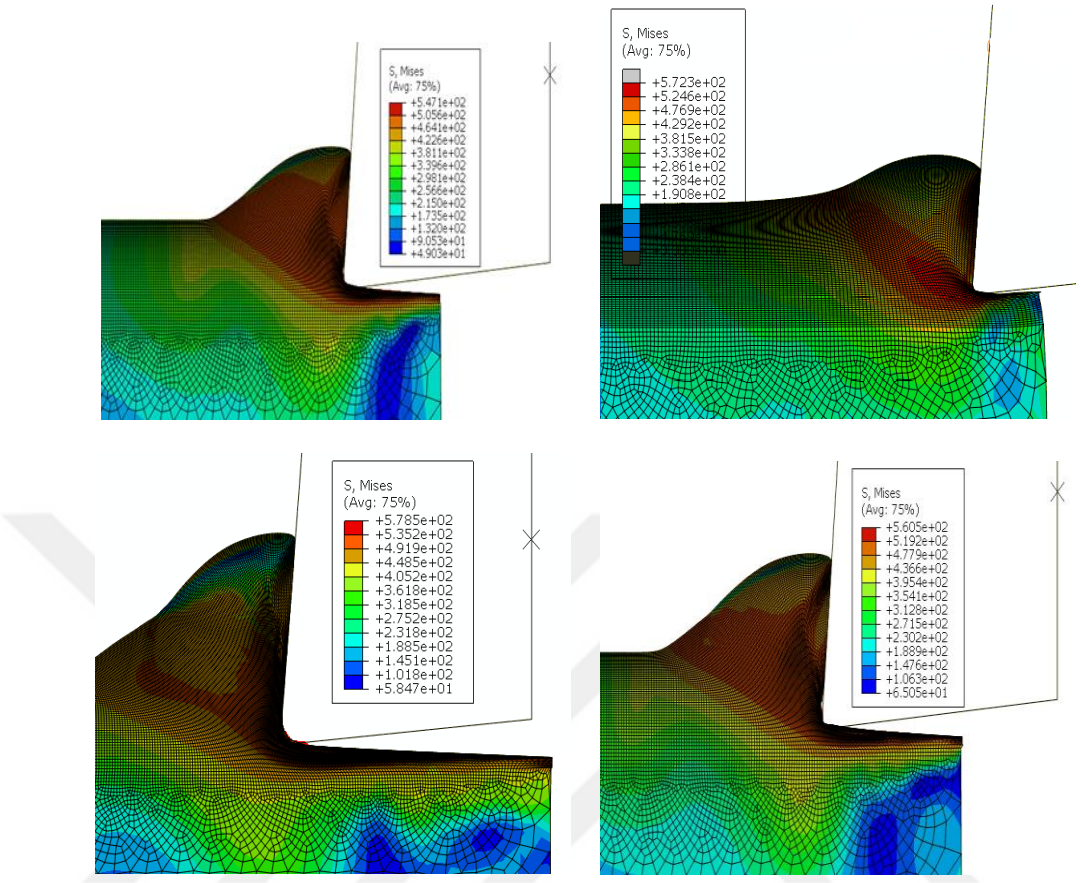

Figure 4.12: Mises Stress distribution obtained from machining simulation of EHM.

A comparison is made for the cutting force of simulated to experimental measurements. The cutting force of EHM is under estimated when compared with experimental. The relative error is 16%.

4.2.2 Model III

In this simulation, the aluminum metal matrix A359 alloy is reinforced in a periodic square particle distribution of SiC 20%. The diameter of these particles is 20 μm. The workpiece and cutting tool material properties are shown in Table 4.8,9 and 10.

Figure 4.13 below shows p-Al-MMC with a periodic square SiC particle distribution.

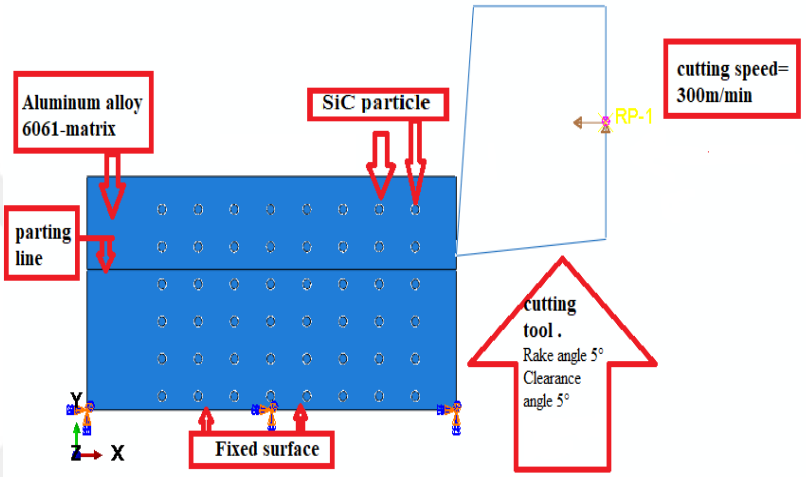

Figure 4.13: FEM of machining Al MMCs with periodic square SiC particle at 20% with diameters of 20 μm.

The cutting condition is shown in Table 4.9 and the cutting tool geometry is shown in Table 4.10.

The chip separation is realized by element deletion method where the chip separation is modeled with using a parting line. For the aluminum matrix, the Johnson and Cook constitutive model is used to include stress variations due to strain, strain rate, and temperature. This relationship is frequently adopted for dynamic problems with high strain rates and temperature effects is shown in Eq.4 at chapter 3.

The Johnson and Cook equation has five material constants, which are *A* for yield stress constant, *B* for strain hardening constant, *n* for strain hardening exponent, *C* for strain rate hardening constant, and *m* for temperature dependency coefficient. T_{room} and T_{melt} are room and melting temperatures, respectively. Johnson-Cook parameters are shown in Table 4.13.

Table 4.13: The Johnson and Cook flow model's parameters [67]

JC parameter	A (MPa)	B (MPa)	C	n	m	T_{room}° C	T_{melt} C
	255	361	0.01	0.18	1.48	20	593

The chip separation is simulated using the Johnson and Cook damage law Eq.5 (chapter 3). The damage was calculated for each element and is defined by Eq.6 (chapter 3).

The parameters for the Johnson and Cook damage law are shown in table 4.12.

The interaction between a particle and a matrix is defined and the interaction of both the matrix and the particle with the cutting tool is defined. A Coulomb friction is used based on the results of experimental [61].

A tie constraint is applied between the particle and the matrix. The contact type is a surface to surface contact.

The load is applied where the cutting tool moves with cutting speed in the x direction and the uncut chip thickness of the cut while the work piece is being fixed.

The Mises Stress distribution obtained from machining simulation of periodic square distribution for p-Al-MMC model are shown in figure 4.14.

The cutting force obtained from machining simulation is compared with the experimental data.

The periodic square particle distribution in the matrix introduced a good agreement with the experimental data with relative error of 8 %.

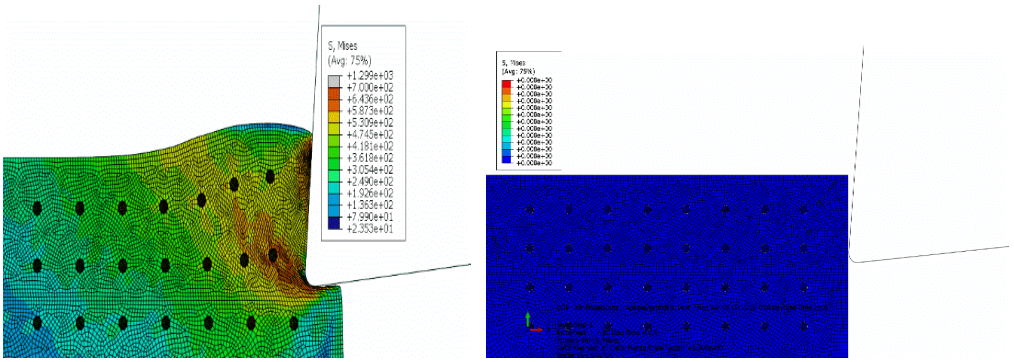

Time = 1.8e–5 sec. Time = 0 sec.

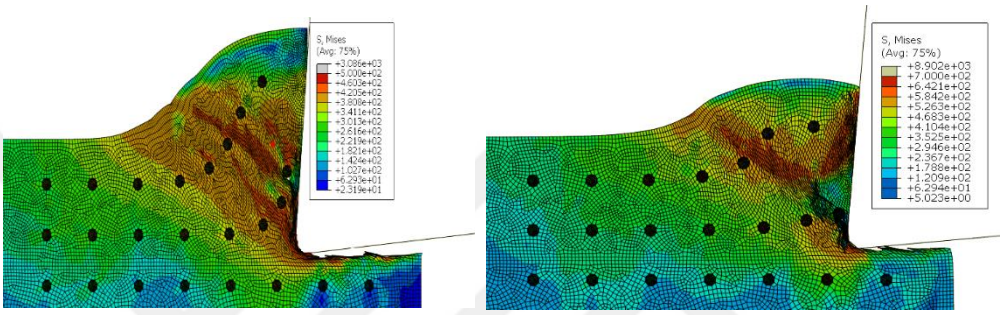

Time = 5.4e–5 sec. Time = 3.6e–5 sec.

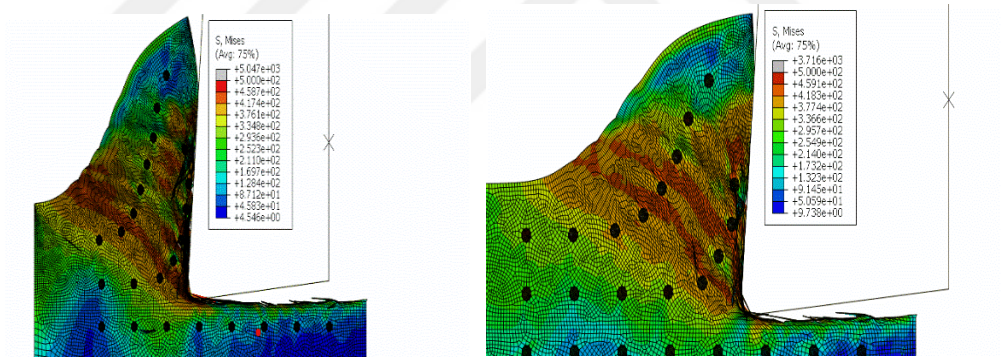

Time = 1.08e–4 sec. Time = 7.2e–5 sec.

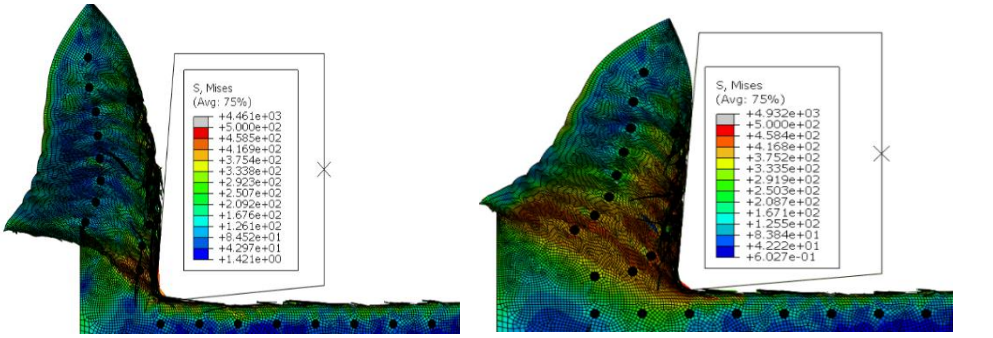

Time = 1.62e–4 sec. Time = 1.26e–4 sec.

Figure 4.14: The Mises Stress distribution obtained from machining simulation of periodic square distribution for p-Al-MMC model.

The simulation in Model III was successful in simulating the interaction between the cutting tool and SiC particles and the interaction between tool and matrix as well as simulating the stress distribution, (Figure 4.15).

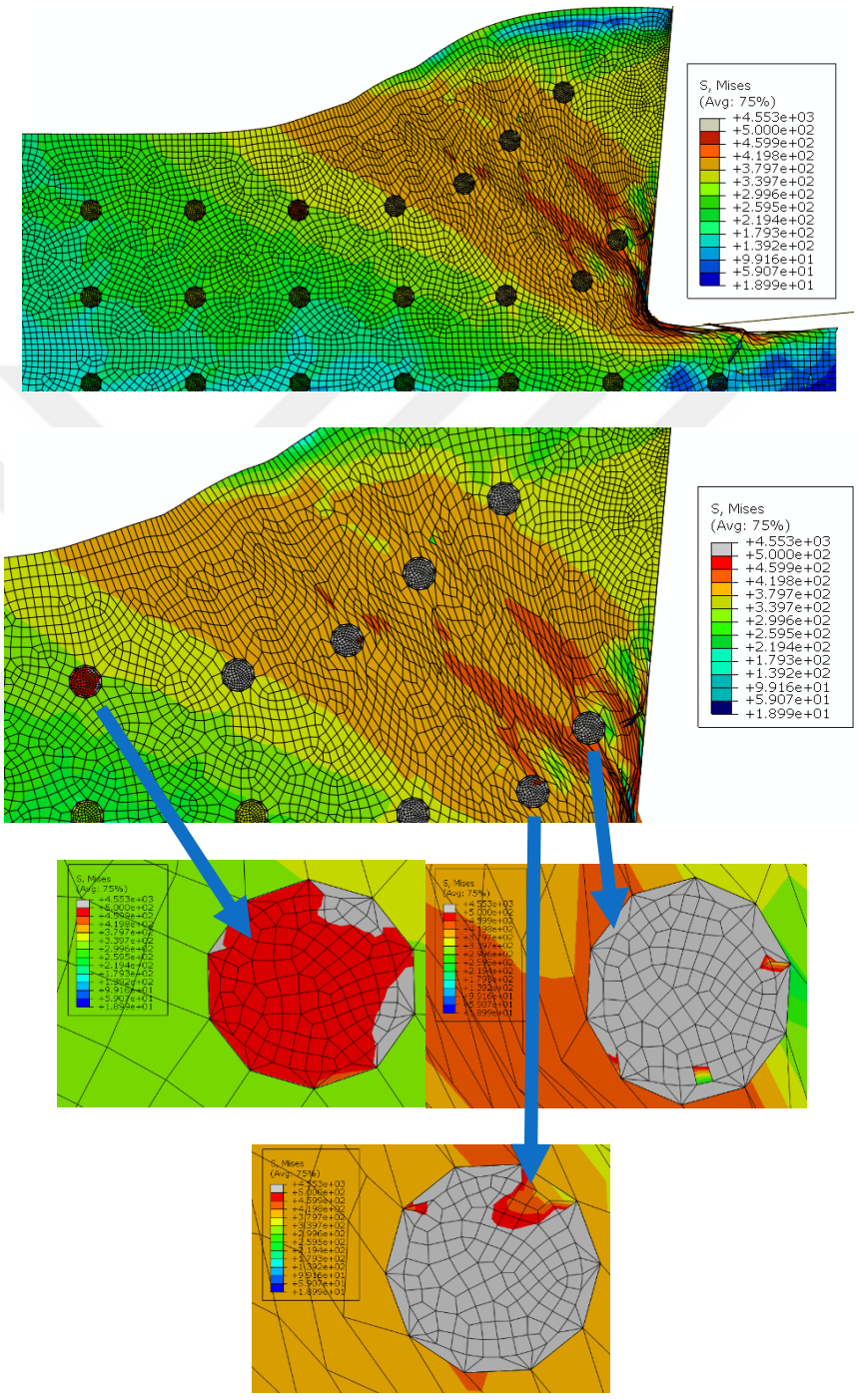

Figure 4.15: Interaction between aluminum matrix and SiC particles and interaction between SiC/Al matrix and cutting tool during the cutting operation (Model III).

4. 2.3 Model IV

In this simulation, the aluminum metal matrix A359 alloy is reinforced with SiC particles. The particles have diameters of 20 μm and a volume fraction of 20%. The distribution of particles is a periodic hexagonal distribution, as shown in Figure 4.16 The cutting condition is shown in Table 4.9 and the cutting tool geometry is shown in Table 4.10.

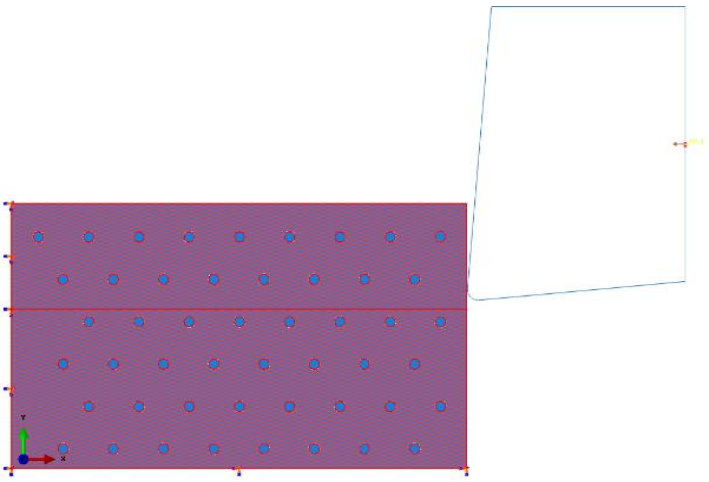

Figure 4.16: Periodic hexagonal distribution model

The chip separation is realized by element deletion method where the chip separation is modeled with using a parting line. For the aluminum matrix, the Johnson and Cook constitutive model is used Eq.4-chapter 3. Johnson-Cook parameters are shown in Table 4.13.

The chip separation is simulated using the Johnson and Cook damage law Eq.5 (chapter 3). The damage was calculated for each element and is defined by Eq.6 (chapter 3).

The parameters for the Johnson and Cook damage law are shown in table 4.12.

The interaction between a particle and a matrix is defined and the interaction of both the matrix and the particle with the cutting tool is defined. A Coulomb friction is used based on the results of experimental [61].

A tie constraint is applied between the particle and the matrix. The type of contact is surface to surface.

The aluminum matrix is assumed as master surface while SiC particle is assumed as a slave surface. The clearance between the two surfaces is zero.

During the cutting process, we notice a large plastic deformation in the aluminum matrix, as shown in Figure 4.17.

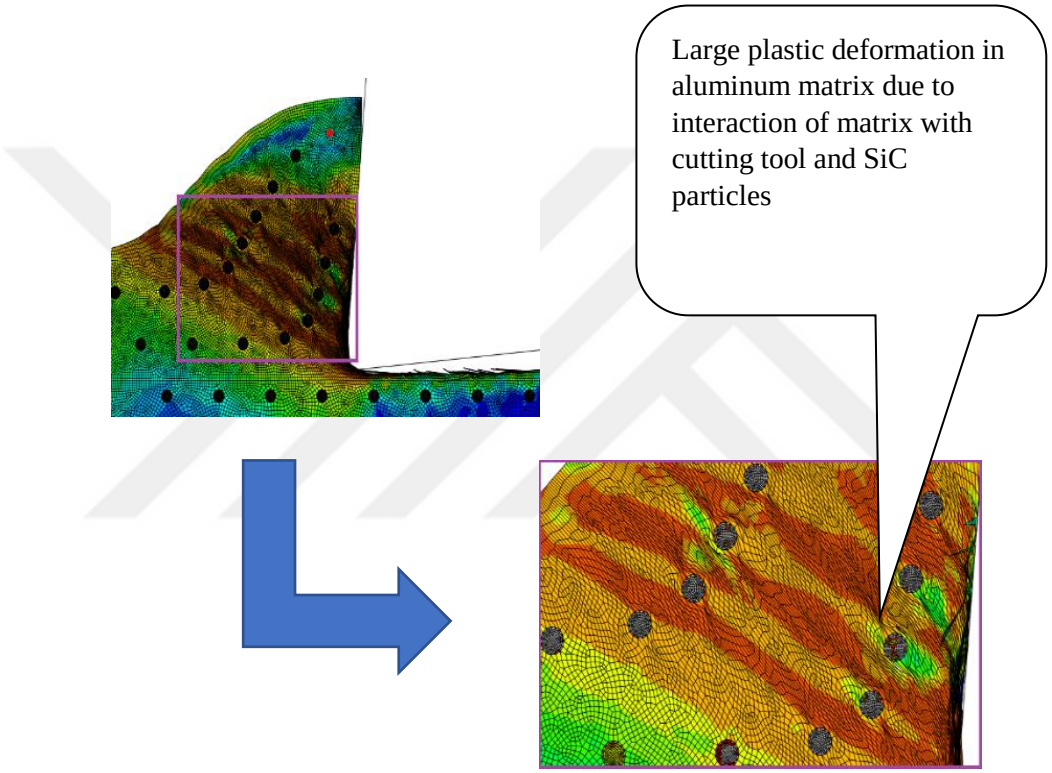

Figure 4.17: Plastic deformation of matrix

The details of machining, stress distribution and chips deformation can be seen in Figures 4.18.

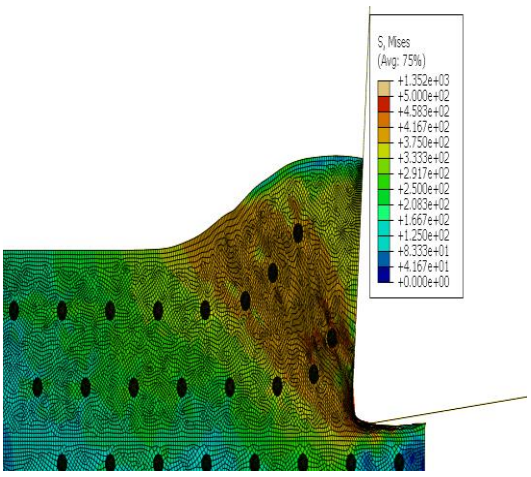

Time = 3e–5 sec.

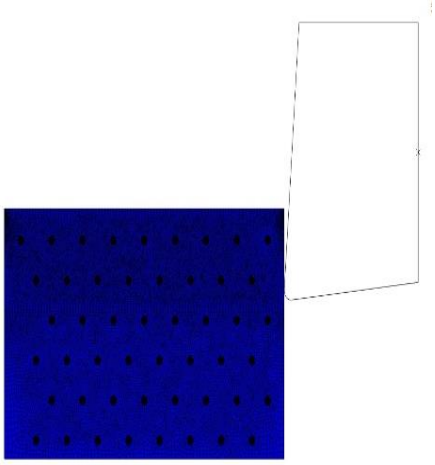

Time = 0 sec.

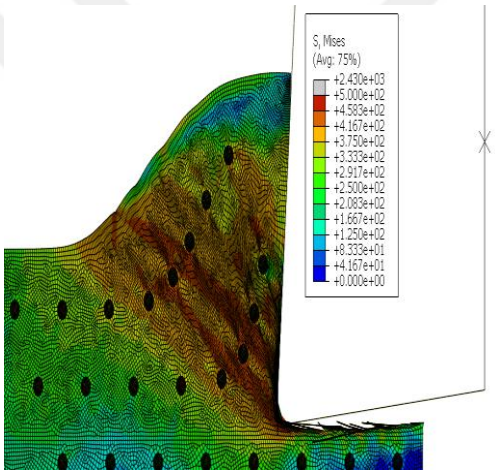

Time = 6e–5 sec

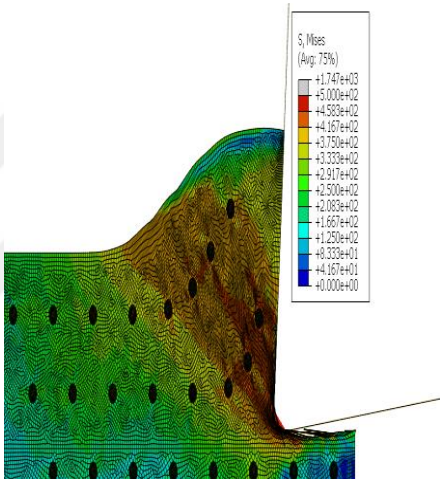

Time = 4e–5 sec.

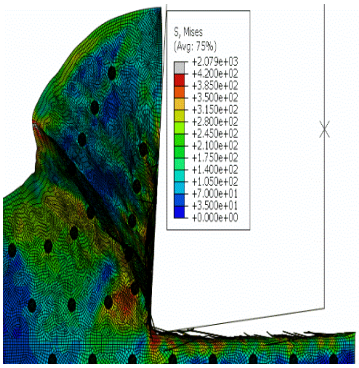

Time = 1e–4 sec.

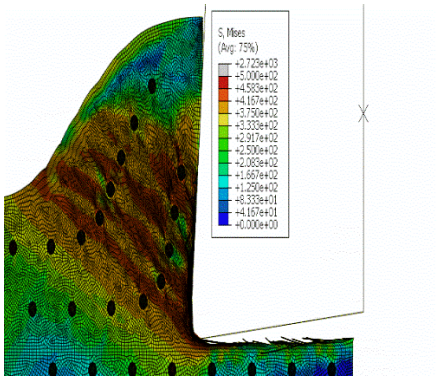

Time = 8e–5 sec.

Figure 4.18: Stress distribution with chips formed using FEM for machining p-Al-MMCs (periodic hexagonal distribution)

This simulation succeeded in producing a cutting force with high accuracy comparable with the experimental data. The relative error of the cutting force is 5.4%.

This simulation gives a clear image about the behavior of p-Al-MMCs during a machining process. A large plastic deformation in the aluminum matrix caused debonding of a number of particles during the machining operation while most of the particles were still bonded in the chips. The interaction between the cutting tool and the SiC particles caused fractures in some of the particles (Figure 4.19).

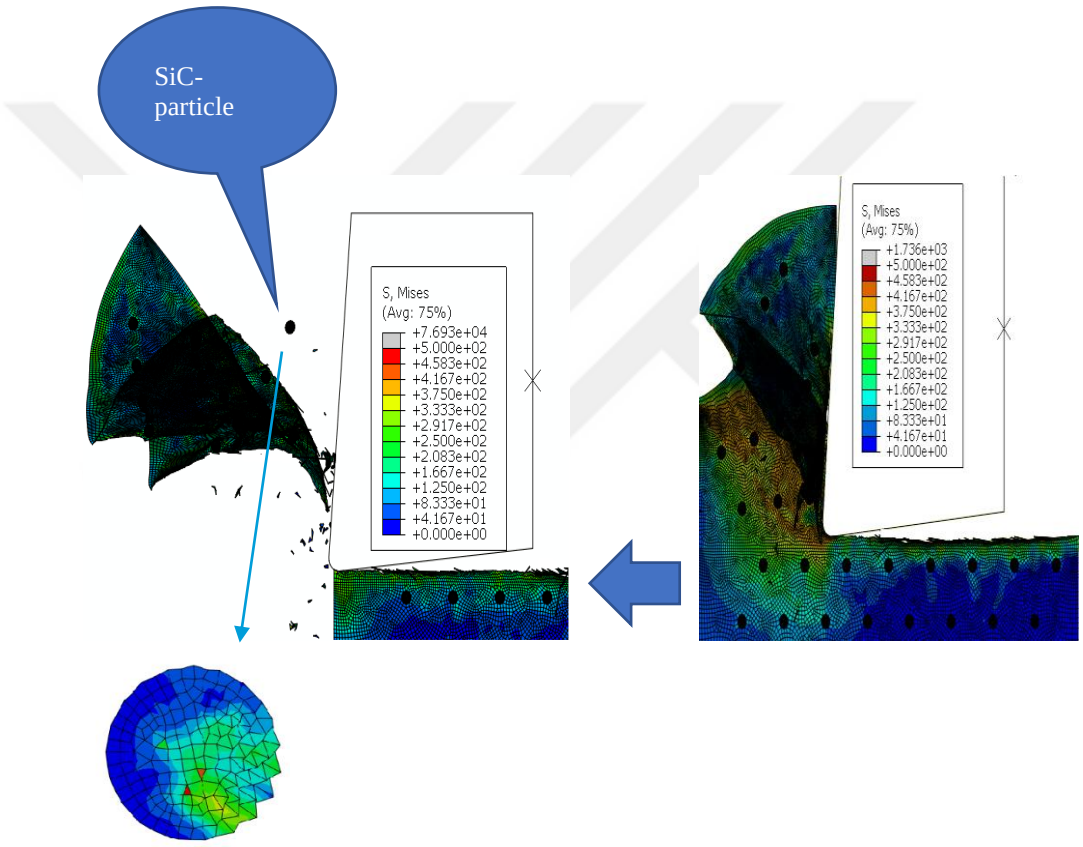

Figure 4.19: Debonding SiC particles from the aluminum matrix.

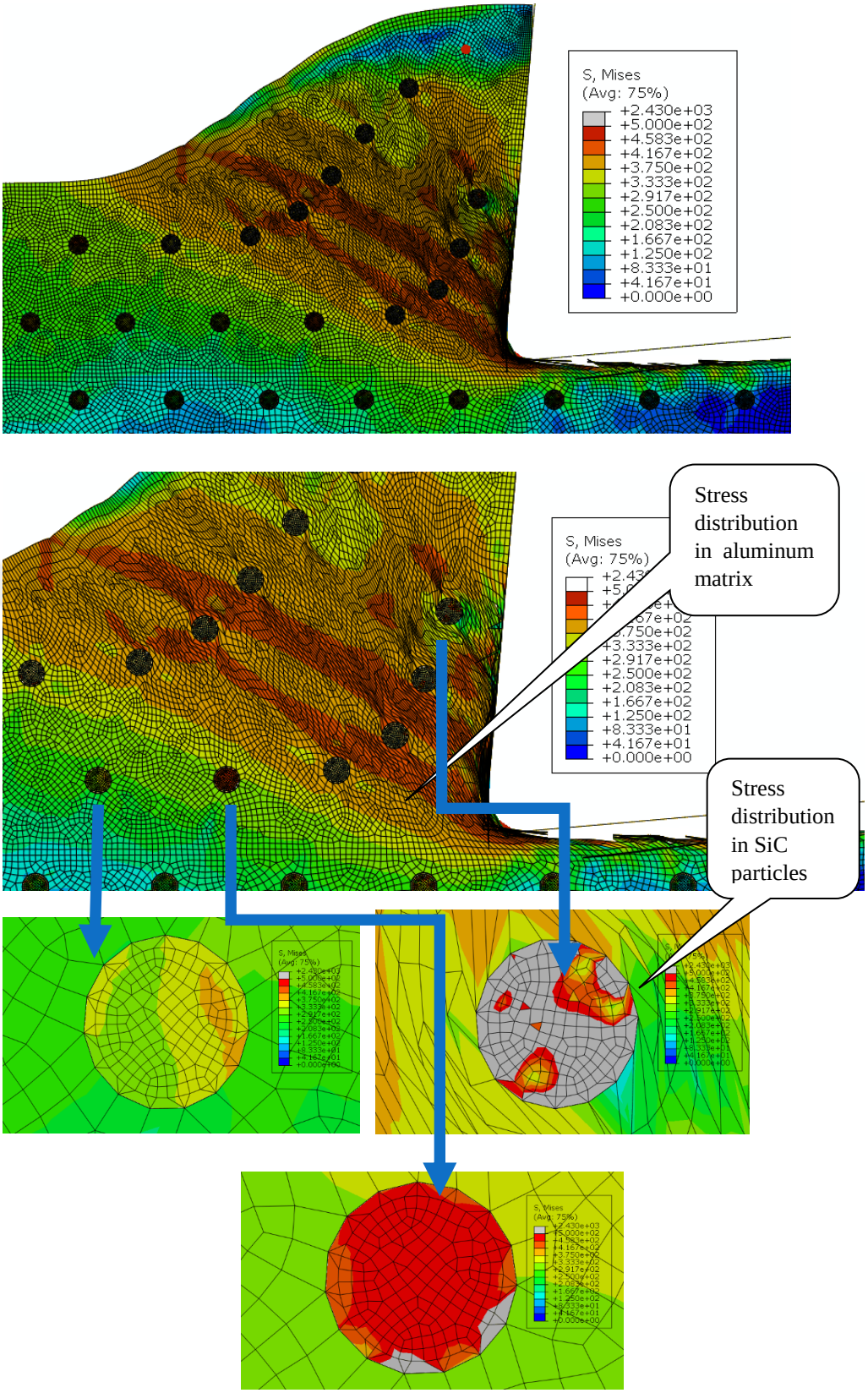

Figure 4.20: Interaction between aluminum matrix and SiC particles and interaction between SiC/Al matrix and cutting tool during the cutting operation – Model IV

4.3 FEM prediction of machining p-Al-MMCs

The cutting force obtained from machining simulation software for three models: Model II (EHM), Model III (periodic square distribution) and Model IV (periodic hexagonal distribution) are summarized in figure 4.21.

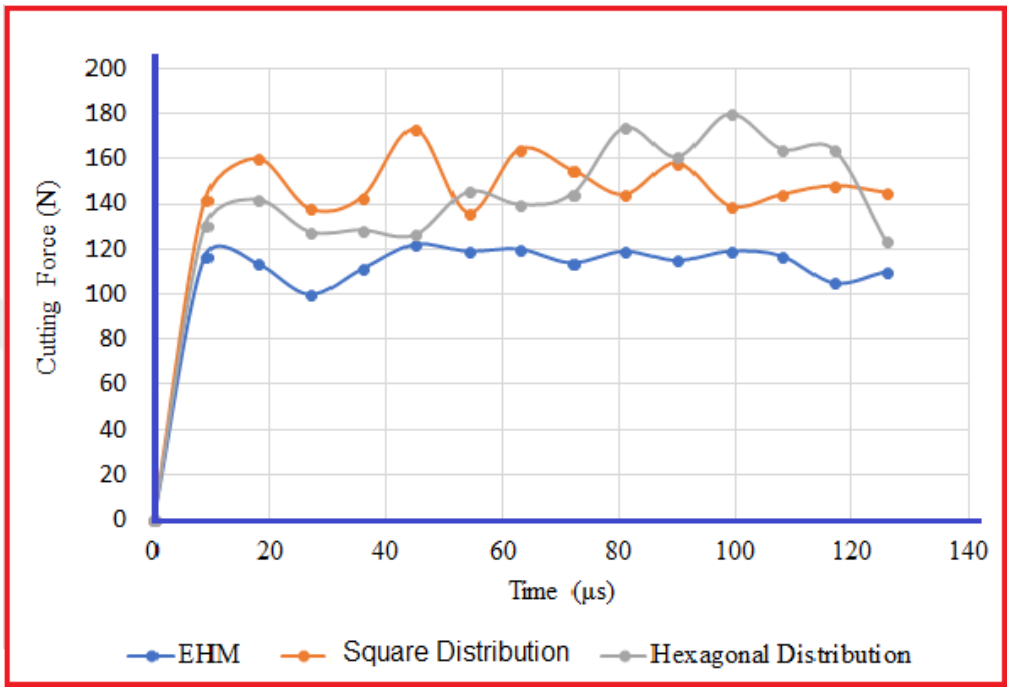

Figure 4.21: Predicted cutting forces with FEM

Comparing the maximum stress distribution for all models of machining p-Al- MMCs in this study.

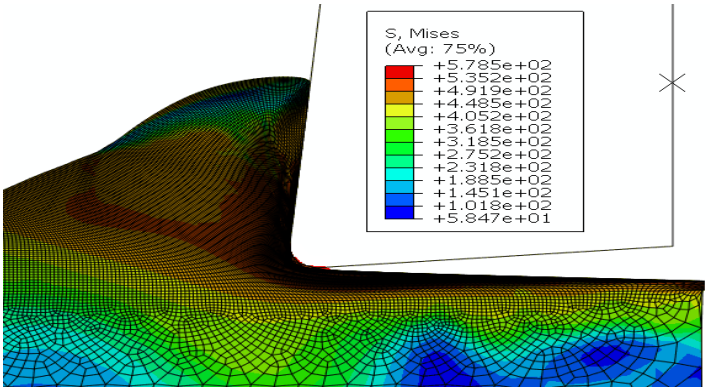

(a) Equivalent homogenous material model (EHM)

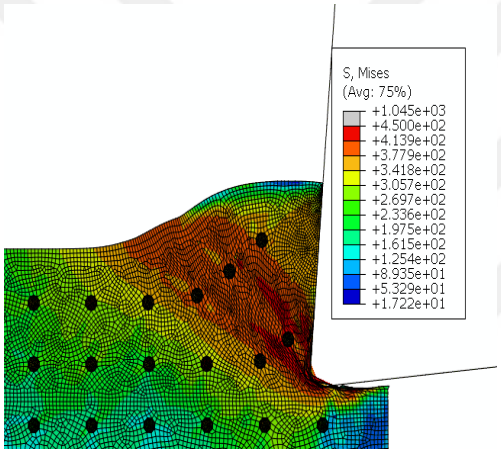

(b) Periodic square distribution

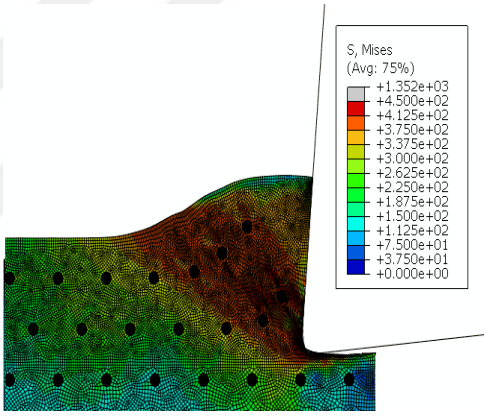

(b) Periodic hexagonal distribution

Figure 4.22: Comparing the maximum Mises stress distributions (MPa) of FEM models

4.4 Results and Discussion

FEM for machining MMC particles is more difficult compared with machining homogeneous materials. Therefore, many approaches are used to describe p-Al-MMCs behavior during machining in this study. The selected matrix material was aluminum alloy A359 reinforced with silicon carbide (SiC) particles having a diameter of 20 μm with a volume fraction of 20%.

The result of three models compared with experimental data, as shown in Figure 4.23. Also, the model for unreinforced matrix material (aluminum alloy A359) added to this compare. This model build depends on Lie and Ramesh experimental and by using Eq.10 and 11 for plastic deformation and Johnson Cook damage for failure (table 4.12).

From the results, it has been found that the FE revealed that modeling p-Al-MMCs as a homogeneous material EHM under estimates machining force about 16%.

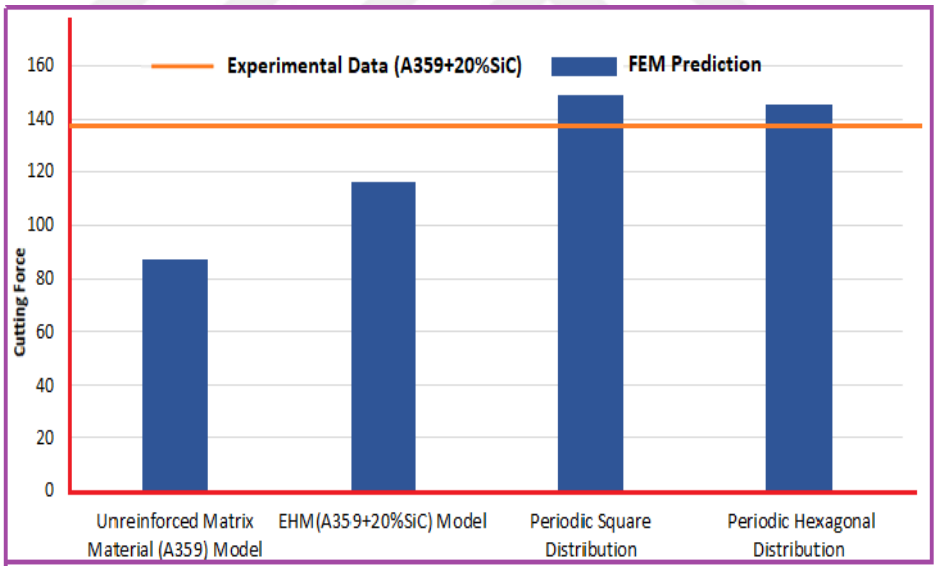

Figure 4.23: FEM predictions compared with experimental data

EHM is not sufficient to predict cutting forces and interaction between matrix with particles and matrix/particle with cutting tool; however, it reduces simulation times.

Both of the heterogenous models the periodic square particle distribution and the periodic hexagonal particle distribution are able to explore particle debonding with plastic deformation in the matrix. In addition, this model

introduced a good accuracy of cutting force compared with experimental data. The periodic square particle distribution in the matrix introduced a good agreement with experimental data with relative error of 8 %.

The periodic hexagonal particle distribution in the matrix introduced the best investigation behavior for the modeling of metal matrix composite (MMC) machining with a relative error of ~5 %.

The stress distribution pattern for EHM is low compared with two heterogenous model. The maximum stress of EHM is ~600 MPa.

The two heterogenous models appear to be very same. Due to the huge differences in the stress level for the reinforcement and matrix, the maximum stress is set to 1300 MPa to better visualize the stress variation in the workpiece matrix.

CHAPTER 5

5. CONCLUSIONS AND SUGGESTIONS FOR FUTURE WORK

5.1 Conclusions

This thesis presents Machining of a Particulate Aluminum Metal Matrix Composite using Finite Element Modeling. This method provides a successful understanding of machining MMCs.

The Abaqus commercial FEM software was used for machining the MMCs.

The FE model was successful in offering an accurate description of MMC behavior while cutting as well as the interactions between the particles with matrix and particle/matrix with the cutting tool. With this method, we were able to find the cutting force required for machining in addition to the stress during this process. Using the finite element, four models were built.

In the first step Model I was built for machining aluminum alloy 6061 during variable cutting conditions in order to establish a reliable finite element model for machining homogenous material.

The simulation results were found to be agreement with experimental results with high accuracy. The investigation indicated that the simulation results are consistent with the experiments. Therefore, the FE simulation method can be used to predict cutting forces accurately during the machining.

The next step was to use FE to build three models to simulate machining of a particulate aluminum metal matrix composites. The selected matrix material was aluminum alloy A359 reinforced with silicon carbide (SiC) particles having a diameter of 20 μm with a volume fraction of 20%. The accuracy of three different modeling approaches to predict machining force was studied. In the first approach, p-Al-MMC was modeled using equivalent homogeneous material (EHM) model where plastic deformation and damage evolution are governed by high-strain rate deformation behavior of a A359/SiC/20p composites and Johnson-Cook damage models, respectively. The cutting force prediction was underestimated with a relative error 16% compared with experimental results. This approach is unable to predict local

effects such as particle matrix interface; nevertheless, it reduced the duration of the simulation. The two models assumed p-AL-MMCs as heterogenous material.

Model III machining assumed that MMCs has a periodic square particle distribution in the aluminum matrix. The cutting force prediction in this model gives a good agreement with experimental results with an error of 8 %.

For the Model IV assumes periodic hexagonal distribution of particles in aluminum matrix. The cutting force prediction with this model is in very good agreement with experimental results with an error of ~5 %.

In the two previous models the interaction between the cutting tool and particles caused fractures in the particles.

Moreover, the interaction between the aluminum alloy and the cutting tool on the first side and the SiC particles on the other side causes a large plastic deformation in the matrix. This deformation causes the particles to deboned from the aluminum matrix while a larger number of particles remains attached to the matrix.

The values of the maximum Mises stress distribution for both the periodic square particle distribution (Model III) and periodic hexagonal particle distribution (Model IV) are very close to each other. In both models, there is a large difference in the Mises stress distribution between the aluminum matrix and the SiC particles. The maximum stress distribution value for the EHM model (Model II) is lowest compared to the above models.

From above, this study finds that the simulation of a periodic hexagonal particle distribution to give the best description of particulate metal matrix composite behavior during the machining process.

5.2 Suggestions for Future Work

SiC particle reinforcement plays an important role in machining MMCs. These particles affect the machining process and cutting forces. All

these criteria can be analyzed using Finite Element Simulation. Therefore, it will be good to deal with the following subjects in future work:

1. Reinforcement Materials: The aluminum matrix can be reinforced with different types of particle, including SiC, $A1_2O_3$ and B_4C. These particles arrange themselves differently at different sizes. This means different mechanical properties with different effects during the machining process. A complex finite element modeling of the MMC machining process can be developed using *Abaqus* or other similar software.

2. Volume Fraction of Reinforcement particle: This value effects machining processes. An increase in fraction volume means more difficulties during machining due to the effect of hard particles while interacting with the cutting tool.

3. Cutting conditions and the type of cutting tool play a major role while machining MMCs. A study on using FEM may focus on:

(a) The effect of different cutting conditions (cutting speed, feed rates and uncut chip thickness) on the behavior of MMCs during machining.

(b) Use FEM to study the effects of reinforcement particles on tool wear or tool life (used deformable cutting tool instead of rigid body).

4. FEM can be applied on fiber-reinforced MMCs and whisker-reinforced MMCs.

5. In this study, we used FEM with two-dimensional orthogonal cutting. A three-dimensional FEM may be developed to study the oblique cutting process for MMCs.

6. Cohesive Zone Modeling could be used to model the interface between the Al matrix and reinforcing particles using FEM.

7. Extending this investigation to other machining operations, such as drilling, milling and boring, will give a more complete overview of the software's potential and also a greater predictive power for further investigation.

Reference

[1] Y. Altintas, Manufacturing Automation: Metal Cutting Mechanics, Machine Tool Vibrations, and CNC Design. Cambridge University Press, 2012.

[2] A. P. Markopoulos, “Finite element method in machining processes”, Springer Science & Business Media, 2012.

[3]MIT,“Cutting Processes I & II,”. [Online]. Available: http://web.mit.edu/2.008/www/lectures/Culpepper-Cutting.pdf.“Orthogonal Machining,” 2010.

[4]http://classes.engr.oregonstate.edu/mime/winter2010/ie337-001/Laboratories/3.

[5] (Source: Childs, et al. (2000)

[6] A.M. Alaskari, S.E. Oraby And H.K. Al-KhalidZ” Mathematical Modeling Experimental Approach of The Friction on The Tool-Chip Interface of Multicoated Carbide Turning Inserts” International Science,2012.

[7] C.K. Aslan “Modelling and simulation of metal cutting by finite element method”, Izmir institute technology, 2009.

[8] L. Filice, F. Micari, S. Rizzuti, and D. Umbrello, “A critical analysis on the friction modelling in orthogonal machining,” Int. J. Mach. Tools Manuf., vol. 47, no. 3–4, pp. 709–714, 2007.

[9]V. Kryzhanivskyy, V. Bushlya, O. Gutnichenko, I. A. Petrusha, and J.-E. Ståhl, “Modelling and Experimental Investigation of Cutting Temperature when Rough Turning Hardened Tool Steel with PCBN Tools,” Procedia CIRP , 2015.

[10] Rawal, S, "Metal-matrix composites for space applications," JOM Journal of the Minerals, Metals and Materials Society,2001.

[11] Kainer, K. U, Metal Matrix Composites -- Custom-made Materials for Automotive and Aerospace Engineering, Wiley-VCH Verlag GmbH & Co. KGaA., 2006.

[12] W. D. Callister, Jr., “Materials Science and Engineering”, John Wiley & Sons, page 400-736, 2008.

[13] M.R.A.Karim ,“Metal matrix composites reinforced with SiC long fibers and carbon nanomaterials produced by electrodeposition”, Politecnico di Toriono, Italy, 2014.

[14] D.L. McDanels // Metall. Trans. A 16 (1985).

[15] B. Vijaya Ramnath1, C. Elanchezhian1, RM. Annamalai1, S. Aravind1, T. Sri Ananda Atreya1, V. Vignesh1 and C. Subramanian,” ALUMINIUM METAL MATRIX COMPOSITES”, 2013.

[16] J.J. Lewandowski and C. Liu, “Effects of Matrix Microstructure and Particle Distribution on fracture of an Al Metal Matrix Composite”, Mat. Sci. Engg., Vol. 107A, pp 241-255,1989.

[17] M.G. McKimpson and T.E. Scott, “Processing and Properties of MMCs Containing Discontinuous Reinforcement”, Mat. Sci. and Engg., Vol. 107A, pp 93-106, 1989.

[18] B. Ralph, H.C. Yuen and W.B. Lee // J. Mater, Proc. Technol,1997.

[19] S.V.S. Narayana Murty, B. Nageswara Rao and B.P. Kashyap, “Composites science and technology “,2003.

[20] J.M. Torralbaa, C.E. da Costab, F. Velascoa, P/M aluminum matrix composites: an overview,2002.

[21] Finnie I., "Review of The Metal Cutting Analyses of The Past Hundred Years",1956.

[22] Taylor F. W, "On the Art of Cutting Metals", Trans. ASME, Vol. 28. 1906.

[23] Shaw MC, "Historical Aspects Concerning Removal Operations on Metals", 1968, In Metal Transformation, Gordon and Breach, New York. MC "The Assessment of Machinability", Proceeding of the Conference on Machinability, Iron and Steel Institute, London,1965.

[24] Ernst, H., and M. E. Merchant, "Chip Formation, Friction and High Quality Machined Surfaces", Surface Treatment of Metals, 194 1.

[25] Kainer, K. U., Metal Matrix Composites -- Custom-made Materials for Automotive and Aerospace Engineering, Wiley-VCH Verlag GmbH & Co. KGaA,2006.

[26] Xia, X., McQueen, H. J., and Zhu, H., "Fracture Behavior of Particle Reinforced Metal Matrix Composites”, Applied Composite Materials, 2002.

[27] Kannan, S., Kishawy, H. A., and Deiab, I., "Cutting forces and TEM analysis of the generated surface during machining metal matrix composites," Journal of Materials Processing Technology, 2009.

[28] Pramanik, A., Zhang, L. C., and Arsecularatne, J. A., "Machining of metal matrix composites: Effect of ceramic particles on residual stress,

surface roughness and chip formation," International Journal of Machine Tools and Manufacture,2008.

[29] T. F. Kfimowicz, "The Large-Scale Commercialization of Aluminum-Matrix Composites", Journal of Material (JOM,1994.

[30] W. Grzesik, Advanced machining processes of metallic materials: theory modelling and applications, 2008.

[31] A. P. Markopoulos," Finite element method in machining processes", Springer Science & Business Media, 2012.

[32] Klamecki, B.E., Incipient Chip Formation in Metal Cutting- A Three Dimension Finite Element Analysis. PhD. Thesis. University of Illinois at Urbana- Champain, 1973.

[33] Ushi, E. and Shirakashi, T. Mechanics of Machining from Descriptive to Predictive Theory. On the Art of Cutting Metals- 75 Years Later, 1982.

[34] Ceretti, E., Fallbohmer, P., Wu, W.T. and Altan, T. Application of 2D FEM to Chip Formation in Orthogonal Metal Cutting. Journal of Materials and Processing Technology, 1996.

[35] Chuzhoy, L., DeVor, R. E., Kapoor, S. G., and Bammann, D. J., "Microstructure- Level Modeling of Ductile Iron Machining," Journal of Manufacturing Science and Engineering, 2002.

[36] A. Ghandehariun, H. M. Hussein& H. A. Kishawy, "Machining metal matrix composites: novel analytical force model" Springer-Verlag London, 2015.

[37] M.V. Ramesh, K.C. Chan, W.B. Lee, C.F. Cheung, Finite-element analysis of diamond turning of aluminum matrix composites, Composites Science and Technology ,2001.

[38] Kishawy, H. A., Kannan, S., and Balazinski, M, "An Energy Based Analytical Force Model for Orthogonal Cutting of Metal Matrix Composites," CIRP Annals - Manufacturing Technology, 2004.

[39] M. Fathipour, P. Zoghipour, J. Tarighi & R. Yousefi," Investigation of Reinforced Sic Particles Percentage on Machining Force of Metal Matrix Composite" ,2012.

[40] A. Ghandehariun1 & M. Nazzal2 & H. A. Kishawy1 & U. Umer," On modeling the deformations and tool-workpiece interactions during machining metal matrix composites", 2016.

[41] A. Pramanik, L.C. Zhang, J.A. Arsecularatne, "An FEM investigation into the behavior of metal matrix composites: tool–particle interaction during orthogonal cutting", 2007.

[42] J. Liua, K. Chenga, H. Dinga, S. Chena, L. Zhaoa "An Investigation of Surface Defect Formation in Micro Milling the 45% SiCp/Al Composite", 2016.

[43] F. Müller and Monaghan, J., "Non-conventional machining of particle reinforced metal matrix composite," International Journal of Machine Tools and Manufacture,2000

[44] J. Chae, Park and T. Freiheit, "Investigation of micro-cutting operations," International Journal of Machine Tools and Manufacture, 2006.

[45] L.A. Looney, J.M. Monaghan, P. O'Reilly, T. Dmrz "The turning of an Al/SiC metal-matrix composite", J Mater Process Technol 33, p 453–468, 1992.

[46] P. J. Arrazola, T. Özel, D. Umbrello, M. Davies, and I. S. Jawahir "Recent advances in modelling of metal machining processes," CIRP Ann. Technol., vol. 62, no. 2, pp. 695– 718, 2013.

[47] T. Özel and Y. Karpat, "Identification of constitutive material model parameters for high-strain rate metal cutting conditions using evolutionary computational algorithms," Mater. Manuf. Process., vol. 22, no. 5, pp. 659–667, 2007.

[48] T. Shirakashi, K. Maekawa, and E. Usui, "Flow stress of low carbon steel at high temperature and strain rate. I: Propriety of incremental strain method in impact compression test with rapid heating and cooling," Bull. Japan Soc., 1983.

[49] J. Lemaitre, A course on damage mechanics. Springer Science & Business Media, 2012.

[50] G. R. Johnson and W. H. Cook, "Fracture characteristics of three metals subjected to various strains, strain rates, temperatures and pressures," Eng. Fract. Mech., vol. 21, no. 1, pp. 31–48, 1985.

[51] T. Mabrouki. Girardin, M. Asad and J.F. Rigal, "Numerical and experimental study of dry cutting for an aeronautic aluminum alloy (A2024-T351)," International Journal of Machine Tools and Manufacture, 48(11), pp. 1187-1197,2008.

[52] C. Muhlstatter, "Calibration and appliance of the Wilkins Damage Model for cast Aluminum' 'Austrian Institute of Technology,2016.

[53] H. Bil, S. E. Kılıç, and A. E. Tekkaya, "A comparison of orthogonal cutting data from experiments with three different finite element models," International Journal of Machine Tools and Manufacture, 44(9), pp. 933-944,2004.

[54] Y. Bao, and T. Wierzbicki, "On the cut-off value of negative triaxiality for fracture," Engineering Fracture Mechanics, 72(7), pp. 1049-1069, 2005.

[55] Y. Bao and T. Wierzbicki, "On fracture locus in the equivalent strain and stress triaxiality space," International Journal of Mechanical Sciences, 46(1), pp. 81-98,2004.

[56] T. Emanuel Fraga da Silva" Numerical Simulation of Metal Cutting Processes Based on DEFORMTM software" University of Porto,2016.

[57] http://www.siso.ch/images/KatalogPage.pdf?k=54

[58] www.united aluminum.com/united-aluminum-alloy-6061

[59] A. A. Dehkharghani, "Tuning Johnson-Cook Material Model Parameters for Impact of High Velocity, Micron Scale Aluminum Particles", Mechanical and Industrial Engineering, Master of Science, Northeastern University Boston, Massachusetts, 2016.

[60] L. E. Schwer, "Aluminum plate preformation: A comparative case study using Lagrange with Erosion…." USA,2009.

[61] C. R. Dandekar, Y. C. Shin "Multi-step 3-D finite element modeling of subsurface damage in machining particulate reinforced metal matrix composites" United States,2009.

[62] A.F. Miranda perez G.Y. Perez Medina, F.J. Garcia Vazquez, A. Arimendi," Wear Resistance Analysis of A359/SiC/20p Advanced Composite Joints Welded by Friction Stir Welding", 2016.

[63] Y. Li, KT. Ramesh, "Comparison of the plastic deformation and failure of A359/SiC and 6061-T6/Al2O3 metal matrix composites under dynamic tension". Mater Sci Eng. 2004.

[64] Y. Li, KT. Ramesh, Chin ESC, "Plastic deformation and failure in A359 aluminum and an A359-SiCp MMC under quasi-static and high-strain-rate tension". J Compos Mater 2007.

[65] M.H. Miguelez, C. Navarro "Dynamic characterization at high temperature of MMCs with discontinuous reinforcement",2000.

[66] W. Mocko, Z.L. Koalewski," Mechanical properties of the A359/SiCp metal matrix composite at wide range of strain rate" Applied mechanical material, Vol.82, P166-171,2011.

[67] U. Umer, M. Ashfaq, J. A. Qudeiri, H. M. A. Hussein, S.N. Danish and A. R. Al-Ahmari," Modeling machining of particle-reinforced aluminum-based metal matrix composites using cohesive zone elements", Springer-Verlag London, 2014.